



УДК 568.152: 551.762.33

A REVIEW OF RUSSIAN UPPER JURASSIC ICHTHYOSAURS WITH AN INTERMEDIUM/HUMERAL CONTACT. REASSESSING *GRENDELIUS* MCGOWAN, 1976

N.G. Zverkov^{1,2*}, M.S. Arkhangelsky^{3,4} and I.M. Stenshin⁵

¹Lomonosov Moscow State University, Leninskie Gory 1, 119991 Moscow, Russia.

²Geological Institute of RAS, Pyzhevski lane 7, 119017 Moscow, Russia; e-mail: zverkovnik@rambler.ru

³Saratov State Technical University, Politekhnikeskaya St. 77, 410054 Saratov, Russia.

⁴Saratov State University, Astrakhanskaya St. 83, 410012 Saratov, Russia.

⁵Ulyanovsk Regional Museum of Local Lore named after I.A. Goncharov, Prospekt Novy Venetz 3/4, 432601 Ulyanovsk, Russia.

ABSTRACT

The Upper Jurassic ichthyosaurs, characterized by the intermedium/humeral contact are known from several localities in Europe and North America. However, they are often described either briefly, or based on fragmentary material, resulting in a taxonomic tangle in most overviews. *Grendelius* McGowan, 1976 was previously synonymized with *Brachypterygius* Huene, 1922. However, it possesses a number of distinct features: intermedium with wide distally faced facet for distal carpal 3 (faced anterodistally in *Brachypterygius* and equal in size with distal carpal 4 facet), posterodistal contact of metacarpal 5 with ulnare (distal in *Brachypterygius*), and absence of postaxial accessory digit (well developed in *Brachypterygius*). We apply a cladistic analysis to place *Grendelius* and *Brachypterygius* in a phylogenetic context. Our analysis recovered *Brachypterygius* and *Grendelius* as distinct groups. The clade *Grendelius* + *Otschevia* gives us good reason to regard the genus *Otschevia* Efimov, 1998 as a subjective junior synonym of *Grendelius*.

Key words: ichthyosaurs, Jurassic, phylogeny, *Brachypterygius*, *Grendelius*

ОБЗОР ПОЗДНЕЮРСКИХ ИХТИОЗАВРОВ РОССИИ, ИМЕЮЩИХ КОНТАКТ ИНТЕРМЕДИУМА И ПЛЕЧЕВОЙ КОСТИ. ПЕРЕСМОТР СТАТУСА РОДА *GRENDELIUS* MCGOWAN, 1976

Н.Г. Зверьков^{1,2*}, М.С. Архангельский^{3,4} и И.М. Стеньшин⁵

¹Московский государственный университет, Ленинские горы, д. 1, 119991 ГСП-1, г. Москва, Россия; e-mail: zverkovnik@rambler.ru

²Геологический институт РАН, Пыжевский переулок 7, 119017 Москва, Россия; e-mail: zverkovnik@rambler.ru

³Саратовский государственный технический университет, ул. Политехническая 77, 410054 г. Саратов

⁴Саратовский государственный университет, ул. Астраханская, 83, 410012 г. Саратов, Россия.

⁵Ульяновский областной краеведческий музей имени И.А. Гончарова, бульвар Новый Венец, 3 /4, 432601, г. Ульяновск, Россия.

РЕЗЮМЕ

Позднеюрские ихтиозавры, обладающие контактом интермедиума и плечевой кости, известны из ряда местонахождений Европы и Северной Америки. Однако их описания зачастую весьма лаконичны, и базируются на фрагментарном материале, что привело к таксономической путанице в ряде обзорных работ. Род

*Corresponding author / Автор-корреспондент

Grendelius McGowan, 1976 раньше считался синонимом рода *Brachypterygius* Huene, 1922, однако он характеризуется рядом признаков: интермедиум с широкой дистально смотрящей фасеткой для III дистальной карпалии (антеродистально направлена у *Brachypterygius* и равна по размерам фасетке для IV дистальной карпалии), постеродистальный контакт V метакarpалии с ульнаре (дистальный у *Brachypterygius*), и отсутствием постаксиального дополнительного пальца (имеется и хорошо развит у *Brachypterygius*). Мы применили кластический анализ для определения филогенетического положения родов *Grendelius* и *Brachypterygius*, в результате получив *Brachypterygius* и *Grendelius* в составе разных клад. Род *Otschevia* Efimov, 1998 вошел в кладу с *Grendelius*, что позволяет нам рассматривать его как младший субъективный синоним рода *Grendelius*.

Ключевые слова: ихтиозавры, юра, филогения, *Brachypterygius*, *Grendelius*

INTRODUCTION

Interest in ichthyosaurs, Mesozoic marine reptiles, has considerably increased in recent years. New genera and species of these fish-like reptiles are annually erected (Fischer et al. 2011, 2012, 2014a, b; Druckenmiller et al. 2012; Roberts et al. 2014; Maxwell et al. 2015), and a number of previously synonymized taxa has been reassessed (Fischer et al. 2014b, 2014c; Arkhangelsky and Zverkov 2014). At present, seven genera of the Upper Jurassic ophthalmosaurids are unambiguously recognized: *Ophthalmosaurus* Seeley, 1874; *Brachypterygius* Huene, 1922; *Nanopterygius* Huene, 1922, *Caypullisaurus* Fernandez, 1997, *Undorosaurus* Efimov, 1999; *Aegirosaurus* Bardet et Fernandez, 2000 and *Arthropterygius* Maxwell, 2010. However, problems regarding the validity and taxonomic position of several Volgian (Tithonian) boreal ichthyosaur genera are still unresolved. These ichthyosaurs are similar to the species described from Western Europe, and, therefore, for a long time they were regarded as subjective junior synonyms of earlier named European forms (Maisch and Matzke 2000; McGowan and Motani 2003; Maisch 2010). Some ichthyosaurs from the Volga Region (*Undorosaurus* Efimov, 1999b, *Paraophthalmosaurus* Arkhangelsky, 1997) differ from their European and American relatives in a number of features (architecture of the forefin and shoulder girdle, the structure of the pelvis, the morphology of the teeth, and so forth). They are most similar to the boreal forms from Svalbard archipelago – *Cryopterygius* Druckenmiller et al., 2012 (Arkhangelsky and Zverkov 2014). The high similarity of Svalbard ichthyosaur *Janusaurus* Roberts et al., 2014 with *Arthropterygius* was discussed by Zverkov et al. (2015). New unpublished data (NGZ) supports wide distribution of *Arthropterygius*-like ichthyosaurs in boreal aquatory.

In this paper we review the peculiar platypterygiine ichthyosaurs, which are characterized by the intermedium/humeral contact. Most of the recent studies (Fischer et al. 2011, 2012, 2014a–c; Roberts et al. 2014; Arkhangelsky and Zverkov 2014) recovered these ichthyosaurs as a sister group to derived Cretaceous platypterygiines. However, the Upper Jurassic platypterygiines are described based on fragmentary material, resulting in a taxonomic tangle in most overviews (Maisch and Matzke 2000; McGowan and Motani 2003; Maisch 2010). Recent discoveries of several new derived ichthyosaurs, elaborated phylogenetic hypothesis of ichthyosaurian interrelationships, and the brevity of the original descriptions of the species “*Otschevia*” *zhuravolevi* Arkhangelsky, 1998 and “*O.*” *alekseevi* Arkhangelsky, 2001 allows us to provide a detailed redescription of these species and reassessment of their phylogenetic position. We also describe a platypterygiine ichthyosaur similar to *Brachypterygius* and *Grendelius*, and combining both primitive and derived features, which suggest its intermediate phylogenetic position.

Phylogenetic analysis recovered *Brachypterygius* and *Grendelius* (= *Otschevia*) as distinct groups: *Grendelius* is recovered as a basal member of Platypterygiinae and *Brachypterygius* as a member of the ‘sveltonectine’ clade (Fischer et al. 2011). We think that these facts confirm validity of both genera.

Institutional abbreviations. BNSS, Bournemouth Natural Science Society (Bournemouth, Dorset, UK); BRSMG, Bristol City Museums and Art Gallery (Bristol, UK); GIN, Geological Institute of the Russian Academy of Sciences (Moscow, Russia); MSU, Lomonosov Moscow State University (Moscow, Russia); MJML, Museum of Jurassic Marine Life (Kimmeridge, Dorset, UK); NHMUK, Natural History Museum (London, UK); SGM, V.I. Vernadsky State Geological Museum of the Russian Acad-

emy of Sciences (Moscow, Russia); SRM, Saratov Regional Museum of Local Lore (Saratov, Russia); SMC, Sedgwick Museum, University of Cambridge (UK); UPM, Undory Paleontological Museum (Undory Village, Ulyanovsk Province, Russia); WESTM, Woodspring Museum, (Weston-super, Mare, UK); YKM, Ulyanovsk Regional Museum of Local Lore named after I.A. Goncharov (Ulyanovsk, Russia).

MATERIAL AND METHODS

For the purpose of this review we examined all the available Upper Jurassic ichthyosaurs referable to Platypterygiinae Arkhangelsky 2001 *sensu* Fischer et al. 2011, deposited in Russian museums (SGM, SRM, YKM).

YKM 56702 – (Fig. 1) incomplete skeleton: fragmentary skull, pectoral girdle, forelimbs, vertebral column, and ribs; Ulyanovsk Province, Ulyanovsk District, Child health center, 18 km north of Ulyanovsk, right bank of the Volga River; Upper Jurassic, Volgian, Dorsoplanites panderi zone.

SRM Hb 30192 – mounted partial skeleton: fragmentary jaw bones, incomplete vertebral column, fragmentary ribs, humeri, epipodial and autopodial elements, right femur; Samara Province, Syzran District, Kashpirskoe Pyroshale Field (Mine № 3); Upper Jurassic, Middle Volgian, lower part of Dorsoplanites panderi zone.

SGM 1445–01 – atlas-axis complex, fragments of presacral centra; SGM 1566 – right coracoid, humerus, elements of epipodium and autopodium; the precise locality of these specimens is unknown; Upper Jurassic, Volgian.

Some samples of rock were collected from the intervertebral space of SGM 1445–01 for microfauna search in order to determine the age of the specimen. The rock, a sandstone with calcareous cement, was disintegrated by using of sodium thiosulfate. The foraminifers selected after a treatment was identified by M.A. Ustinova (GIN) as *Saracenaria prolata* K. Kuznn and *Lenticulina* sp., which allows attributing the bones to the Middle Volgian, Upper Jurassic (possibly Dorsoplanites panderi zone).

SGM 1445–01 and SGM 1566 have different collection numbers, because they were placed in different trays and were numbered at different times. However, bone preservation and lithology of the matrix confirm their unity. Additionally, X-ray phase analysis was carried out by V.L. Kosorukov (Department of lithology,

MSU) to test the unity of the matrix SGM 1445–01 and SGM 1566. The results revealed that the mineral composition and the proportion of mineral phases in the selected samples are very similar.

The terms for the regions of the vertebral column follow Kirton (1983) and McGowan and Motani (2003). Because cervical and dorsal vertebrae are indistinguishable in ichthyosaurs, the neutral term ‘presacral’ is used for all vertebrae, located caudally to atlas-axis complex and possessing diapophyses and parapophyses.

Phylogenetic analysis. To determine the phylogenetic relationships of the genera *Grendelius* and *Brachypterygius*, as well as their position within Ichthyosauria, an analysis was conducted on the basis of 26 taxa and 61 characters (Appendix 1). We use the matrix developed by Fischer et al. (2012) and several characters were taken from Arkhangelsky and Zverkov (2014), Sander (2000) and Roberts et al. (2014) (see Appendix 2). *Temnodontosaurus* is used as an outgroup in our analysis. Coding of some characters for *Mollesaurus periallus* Fernandez, 1999, *Arthropterygius chrisorum* (Russell, 1993) and *Caypullisaurus bonpartei* Fernandez, 1997 were changed in accordance with new data (Fernández 2007; Fernández and Talevi 2013; Roberts et al. 2014). (See Appendices 1 and 3). In addition, we added three taxa to the analysis: *Grendellius pseudoscythicus*, *G. zhuravlevi*, and *G. alekseevi* (all three species were previously referred to the genus *Otschevia*). We treated *Grendelius mordax* and *Brachypterygius extremus* as distinct operational taxonomic units (OTUs), while these were combined in a single OTU by Fischer et al. (2012) under the name *Brachypterygius extremus*, following McGowan (1997).

Two new characters (7 and 27), relating to morphology of the atlas-axis complex and nasal, were added to the matrix (see Appendix 2). The new characters were coded based on the literature (Gilmore 1905; Andrews 1910; Appleby 1956; Johnson 1979; Wade 1984, 1990; Delair 1986, 1987; Arkhangelsky 1997, 1998a, b; Kirton 1983; Fernández 1994, 1997, 1999, 2001, 2007; Efimov 1997, 1998, 1999a, b; Bardet and Fernández 2000; McGowan and Motani 2003; Kear 2005; Maxwell and Caldwell 2006; Kolb and Sander 2009; Druckenmiller and Maxwell 2010; Maxwell 2010; Fischer et al. 2011, 2012, 2013; Druckenmiller et al. 2012; Fischer 2012; Fernández and Talevi 2013). Three different specimens (NHMUK R3177, SMC J68516 and BRSMG Ce 16696), originally encoded

by Fischer et al. (2012) as a single OTU of *Brachypterygius extremus*, were considered in the following way: *Grendelius mordax* (OTU1) integrating SMC J68516 and BRSMG Ce 16696 based on practically identical cranial morphology (McGowan 1997) and *Brachypterygius extremus* (OTU2) based on the holotype specimen (NHMUK R3177) and materials with a high degree of probability belonging to the same individual (WESTM 78/219 and BNSS 0006). Encoding of *G. mordax* was supplemented by authors personal observations based on photographs of the holotype SMC J68516 and BRSMG Ce 16696 kindly provided by B.C. Moon (pers. com. May 2014) and V. Fischer (pers. com. July 2015). The data matrix was processed in TNT ver.1.1. (Goloboff et al. 2008), using the heuristic search via the Wagner algorithm, 1000 replications, tree bisection and reconnection branch swapping, 10 trees save per replication.

SYSTEMATICS

Order Ichthyosauria de Blainville, 1835

Family Ophthalmosauridae Baur, 1887

Subfamily Platypterygiinae Arkhangel'sky, 2001 *sensu* Fischer et al. 2012

Genus *Brachypterygius* Huene, 1922

Brachypterygius extremus (Boulenger, 1904)

Ichthyosaurus extremus: Boulenger, 1904: 425.

Brachypterygius extremus: Huene, 1922: 97.

Holotype. NHMUK R3177, an associated forefin. Precise locality and age are unknown (see discussion).

Revised diagnosis. Modified from Huene (1920) and Kirton (1983); supplemental characters: a medium-sized (up to 4 m judging by the forelimb length) platypterygiine ichthyosaur, possessing the following unique combination of features: humerus with three distal facets (the middle facet being smaller than the other two and articulating with the intermedium, which wedges between radius and ulna); anterodistal edge of the humerus protruding anteriorly and practically forming a contact with the first element of the anterior accessory digit; equal intermedium facets for the distal carpals 3 and 4; reduced contact of intermedium and radiale; absence of contact between pisiform and metacarpal 5; rectangular and tightly packed proximal autopodial elements.

Comparison. *Brachypterygius extremus* differs from other platypterygiine genera in expanded forelimb, wherein the intermedium equally contacts with distal carpals 2 and 3, and enlarged pisiform. It is similar to *Aegirosaurus*, *Grendelius* and *Maiaspondylus* Maxwell et Caldwell, 2006 in the presence of the intermedium/humeral contact; to *Sveltonectes* Fischer et al., 2011 in the reduced contact of intermedium/radiale; and to *Aegirosaurus*, *Sveltonectes*, *Platypterygius hercynicus* Kuhn, 1946 in the strong development of one posterior accessory digit. A small amount of phalanges in the digits could be a result of incorrect mounting during preparation (Kirton, 1883). If such a small amount of phalanges was a natural condition (Delair, 1986), it could be an additional unique feature of *Brachypterygius extremus*.

Remarks. Diagnosis for the genus as for the type species.

Genus *Grendelius* McGowan, 1976

Grendelius: McGowan, 1976: 671; Kirton, 1983: 110.

Brachypterygius: Maisch and Matzke, 2000: 79; McGowan and Motani, 2003: 117; Maisch, 2010: 166.

Otschevia: Efimov, 1998: 82; Motani, 1999: 485; Storrs et al, 2000: 202; Arkhangel'sky, 2001: 69; 2008: 252.

Type species. *Grendelius mordax* McGowan, 1976; Upper Jurassic, Lower Volgian (Tithonian); Norfolk, United Kingdom.

Other species. *Grendelius zhuravlevi* (Arkhangel'sky, 1998), comb. nov.; Upper Jurassic, Middle Volgian, Saratov and Samara provinces, Russia; *Grendelius pseudoscythicus* (Efimov, 1998), comb. nov., Upper Jurassic, Lower Volgian; Ulyanovsk Province, Russia; *Grendelius alekseevi* (Arkhangel'sky, 2001), comb. nov.; Upper Jurassic, Middle Volgian; Ulyanovsk Province, Russia.

Distribution. Upper Jurassic, Lower Volgian (Tithonian), United Kingdom; Lower to Middle Volgian, Russia; ?Upper Tithonian, Mexico (Buchy and López Oliva 2009).

Revised diagnosis. Modified from McGowan (1976), Kirton (1983), Efimov (1998), and Arkhangel'sky (2000, 2001); supplemental characters based on authors personal observations: a medium-sized platypterygiine ichthyosaur possessing the following unique combination of features: massive skull with long robust jaws and relatively small eyes; prominent hump on internasal surface of the nasal just before

the beginning of the excavatio internasalis; rostrally protruding process on the dorsal border of the nares, overlapping premaxilla externally (unambiguous autapomorphy, character 7, state 1); wide, sheet-like sub- and supranarial processes on the premaxilla (autapomorphy); deep concavity on the dorsal border of the lacrimal, surrounded anteriorly and posteriorly by ridges and participating in the ventral border of the external nares (autapomorphy); basioccipital lacking a basioccipital peg, with the condyle not clearly set off from the extracondylar area, the latter being extremely reduced; robust interclavicle with spade shaped posterior process expansion; humerus with three or four distal facets, the medial one is for contact with intermedium, the posterior 4th – for neomorphic ossicle; ulnare excluded from contact with the intermedium by distal carpal 4 and contacts distally metacarpal 4; intermedium possessing wide distal contact with distal carpal 3; metacarpal 5 contacts ulnare posterodistally; femur with two distal facets and prominent dorsal and ventral processes; tibial facet twice smaller than fibular facet.

Comparison. *Grendelius* differs from other ophthalmosaurids in presence of the process on the dorsal border of the nares, externally overlapping premaxilla, and deep concavity on the dorsal border of the lacrimal, participating in the ventral border of the external nares. The spade shaped posterior expansion of the interclavicle is similar to that of *Cryptopterygius* (Druckenmiller et al. 2012). *Grendelius* differs from sveltonectine ichthyosaurs (clade ‘S’, see discussion) by the robust skull with large teeth. In a wide distal contact of intermedium with distal carpal 3 and posterodistal contact of metacarpal 5 with ulnare *Grendelius* is similar to *Undorosaurus* (Efimov 1999b; Arkhangelsky and Zverkov 2014), *Cryptopterygius* (Druckenmiller et al. 2012; Arkhangelsky and Zverkov 2014), *Paraophthalmosaurus* (Efimov 1999a; Arkhangelsky and Zverkov 2014), *Caypullisaurus* (Fernández 1997, 2001), *Platypterygius* (e. g. Arkhangelsky et al. 2008; Kolb and Sander 2009; Maxwell and Kear 2010; Zammit et al. 2010) and different from *Brachypterygius*, *Sveltonectes* (Fischer et al. 2011) and *Ophthalmosaurus* (Andrews 1910; Applebey 1956). Absence of postaxial (6) digit, observed also in *Undorosaurus* and *Cryptopterygius* (Efimov 1999b; Druckenmiller et al. 2012; Arkhangelsky and Zverkov 2014), distinguishes *Grendelius*, *Undorosaurus* and *Cryptopterygius* from all other Upper Jurassic and Cretaceous ophthalmosaurids.

***Grendelius mordax* McGowan, 1976**

Grendelius mordax: McGowan, 1976: 671, figs. 1; 2A, B, C, F; 3.

Brachypterygius mordax: Maisch and Matzke, 2000: 79; Maisch, 2010: 166.

Brachypterygius extremus: McGowan and Motani, 2003: 117, fig. 94.

Holotype SMC J68516, a complete skull with associated postcranial elements; United Kingdom, Norfolk, Great Ouse Flood Relief Channel, about 100 m south of the bridge at Stowbridge, 12 km south of King’s Lynn, Upper Jurassic, Early Volgian (Tithonian), Pectinatites wheatleyensis zone.

Distribution. Volgian (Tithonian), Upper Jurassic, Stowbridge, Norfolk; Kimmeridge Bay, Dorset, United Kingdom.

Referred specimens. Holotype SMC J68516; BRSMG Ce 16696 (a partial skeleton), United Kingdom, Dorset, Kimmeridge Bay; Upper Jurassic, Volgian (Tithonian).

Revised diagnosis. Modified from McGowan, 1976, 1997; McGowan and Motani 2003; supplemental characters based on authors personal observations: a medium-sized platypterygiine ichthyosaur possessing the following autapomorphies: ulnare excluded from contact with intermedium by distal carpal 4 and distally contacting metacarpal 4; intermedium possessing distal contact with distal carpal 3 and posterodistal contact with metacarpal 4; oval and thickened autopodial elements.

Comparison. The cranial morphology of *G. mordax* is very similar to *G. alekseevi*, while differs in more robust and ventrally convex parasphenoid base and presence of prominent hypoglossal foramina in the exoccipital. The forefin architecture of *G. mordax* differs from other *Grendelius* species in presence of intermedium and distal carpal 4 contact and absence of additional ossicles. Detailed comparison is difficult due to absence of detailed description for BRSMG Ce 16696.

***Grendelius alekseevi* (Arkhangelsky, 2001), comb. nov.**

Otschevia alekseevi Arkhangelsky, 2001: 66, figs. 1–3; Arkhangelsky, 2008: 252, fig. 7.

Brachypterygius alekseevi: Maisch, 2010: 167.

Holotype YKM 56702; partial skeleton: fragmentary skull, humeral girdle, forelimbs, vertebral col-

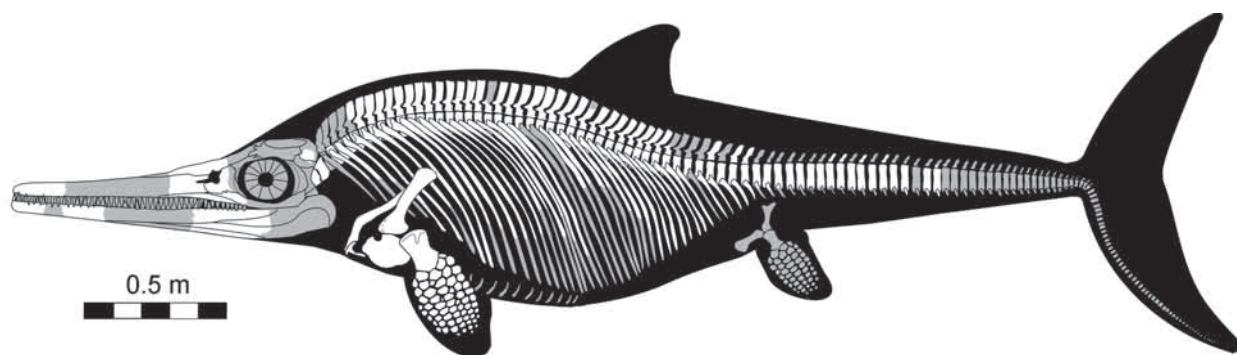


Fig. 1. Skeletal reconstruction of *Grendelius alekseevi* based on some cranial and postcranial features of *Grendelius mordax* and *Brachypterygius extremus*. Presented skeletal elements are marked by white.

umn and ribs (Fig. 1); Russia, Ulyanovsk Province, Ulyanovsk District, Child health center, 18 km north of Ulyanovsk, right bank of the Volga River; Upper Jurassic, Middle Volgian, Dorsoplanites panderi zone.

Revised diagnosis. A medium-sized ichthyosaur, characterized by the following autapomorphies: wide and squat exoccipital with reduced basal anterior process; medial part of the scapula gradually expanded anteroposteriorly; reduced humeral torsion; four distal humeral facets with the posterior one for a neomorphic ossicle; flattened and plate-like zeugo- to autopodial elements (character 51, state 0); two preaxial accessory digits; neomorphic ossicles convergent to centralia, located anterodistally to intermedium and separating the contact of radiale and distal carpal 3.

Description. Measurements of YKM 56702 are given in Table 1.

Skull. The skull is not fully preserved. There are fragments belonging to the area of the external nares, basisphenoid, basioccipitale, both stapedes and quadrate bones, incomplete jugal and postorbital, strongly deformed fragments of the skull roof, fragment of the supraoccipital, fragments of the upper and lower jaws in the material.

The bones forming the region of the left external naris are slightly disarticulated relative to each other and their natural contacts are altered. This condition changes outline of the naris. The bones participating in the narial region form the depression around the external naris.

The *maxilla* extending far anteriorly but not as far as the nasal (Fig. 2). Its preserved fragment is laterally compressed; it forms the internal part of the labial wall and the dorsal part of the deep dental

groove. The maxilla seems to form the process on the ventral border of the naris; however, it is difficult to distinguish because of poor preservation of the bone in this region. Posterolaterally, maxilla is covered by a small fragment of the jugal anterior margin expansion (Fig. 2).

The dorsal surface of the *nasal* is thick, forming the hump just before the beginning of the excavatio internasalis. The nasal bone overhangs the nostril dorsally. A thin, short lateral wing originates above the posterodorsal margin of the external naris. Anteriorly the nasal forms a process on the dorsal border of the naris, which protrudes rostrally and covers externally the sheet-like process supranarialis of the premaxilla (Fig. 2) – autapomorphy of *Grendelius*.

The anterior part of the *lacrimal* is preserved. The dorsal edge of the lacrimal participates in the ventral and posterior borders of the external nares. In the middle part, it bears a deep concavity, which is reflected inwards and surrounded anteriorly and posteriorly by the ridges. The anterior margin of the lacrimal is folded, forming an interdigitating suture with the maxilla; the ventral margin of the bone connects with the maxilla by straight suture (Fig. 2).

The preserved portion of the *premaxilla* is broken by a long anteroposterior fissure. Towards its posterior margin, it shows the presence of wide and short, sheet-like processes subnarialis and supranarialis (Fig. 2). The posterior edge of the premaxilla is incised by a thin notch forming the anterior border of the external nares. The lateral surface of the premaxilla bears a deep longitudinal groove that commence immediately at the posterior edge of the bone.

The *quadrate* (Fig. 3K–M) is a large ‘C’-shaped bone consisting of an anteromedially orientated ptery-

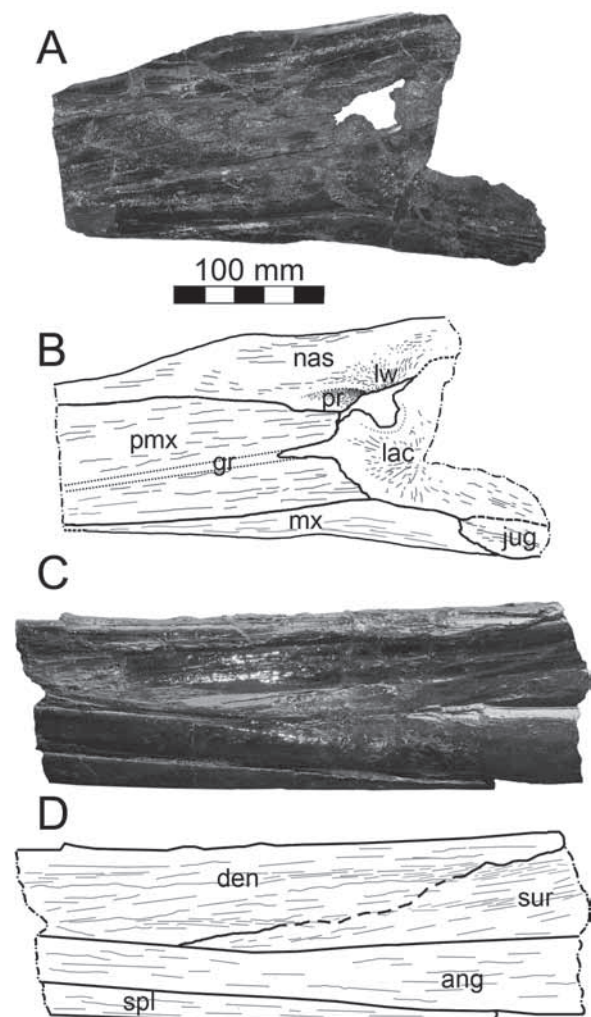
Table 1. Selected measurements (mm) of the holotype (YKM 56702) of *Grendelius alekseevi* (see Fig. 3 for abbreviations used; for postcranial measurements see Arkhangelsky 2001).

Bone	Length	Width	Height	Measurements
Basioccipital	82	97	79	exa. width 17; fm. width 12; fst. heigh 40; fop. height 20; fex. length 35
Basishenoid	89	anterior 131; posterior 68	anterior 67; posterior 50	icf. diameter 11; fst length 50
Quadrate	dorsal 70; ventral 100	acond. 67	150	length in the area of quadrate foramen 65
Stapes	mediolateral 96	occipital head 67	occipital head 63	–
Atlas-axis	55	90	88	–

goid lamella and posterolaterally orientated occipital lamella. The ventral surface of the massive condyle is divided anteriorly by the smooth groove. This groove separates bosses for the articulation with the articular (from a medial part) and for the articulation with the surangular (from a lateral part). The lateral part forms a prominent bulge posterodorsally. The stapedial facet is slightly concave. It is located near to the ventral end of the bone. The anterior pterygoid lamella is plate-like and bears a groove along its anterior margin. The lateral edge of the quadrate is emarginated by the large quadrate foramen. Immediately above the condylar surface, the lateral edge of the quadrate bears a facet for the quadratojugal (Fig. 3L, M).

The *basioccipital* (Fig. 3A–C) is a massive spherical bone with hemispherical occipital condyle and extremely reduced extracondylar area. The notch-like notochordal pit indents the condylar surface in dorsal half of the condyle just under the foramen magnum (Fig. 3A). The base of the foramen magnum forms a shallow embayment on the dorsal surface of the condyle (Fig. 3B), laterally restricted by wide rounded facets for the exoccipital. The shallow floor of the foramen magnum forms anteriorly emerging basioccipital peg (Fig. 3B). The stapedial facets are circular in outline; they are located in the ventral part of the anterolateral surfaces of the basioccipital. The opisthotic facets are comparable in size to the stapedial facets and located in the anterodorsal surfaces of the basioccipital (Fig. 3C).

The *basisphenoid* (Fig. 3B–E) is a massive isometric bone, pentagonal in dorsal view and trapezoidal in lateral view. In the posterior part, it extensively contacts the basioccipital. The dorsal pitted surface of the basisphenoid is posteromedially inclined contributing to a deep nerve channel passing between the opisthotic and stapes. The basiptyergoid

**Fig. 2.** The region of the external naris and the fragment of the left mandible of *Grendelius alekseevi* YKM 56702: A, C – photographs; B, D – interpretive drawings. Abbreviations: ang – angular; den – dentary; gr – fossa praemaxillaris; jug – jugale; lac – lacrimale; lw – lateral wing; mx – maxilla; nas – nasale; pmx – premaxilla; pr – process of the narial bulge; spl – splenial; sur – surangular.

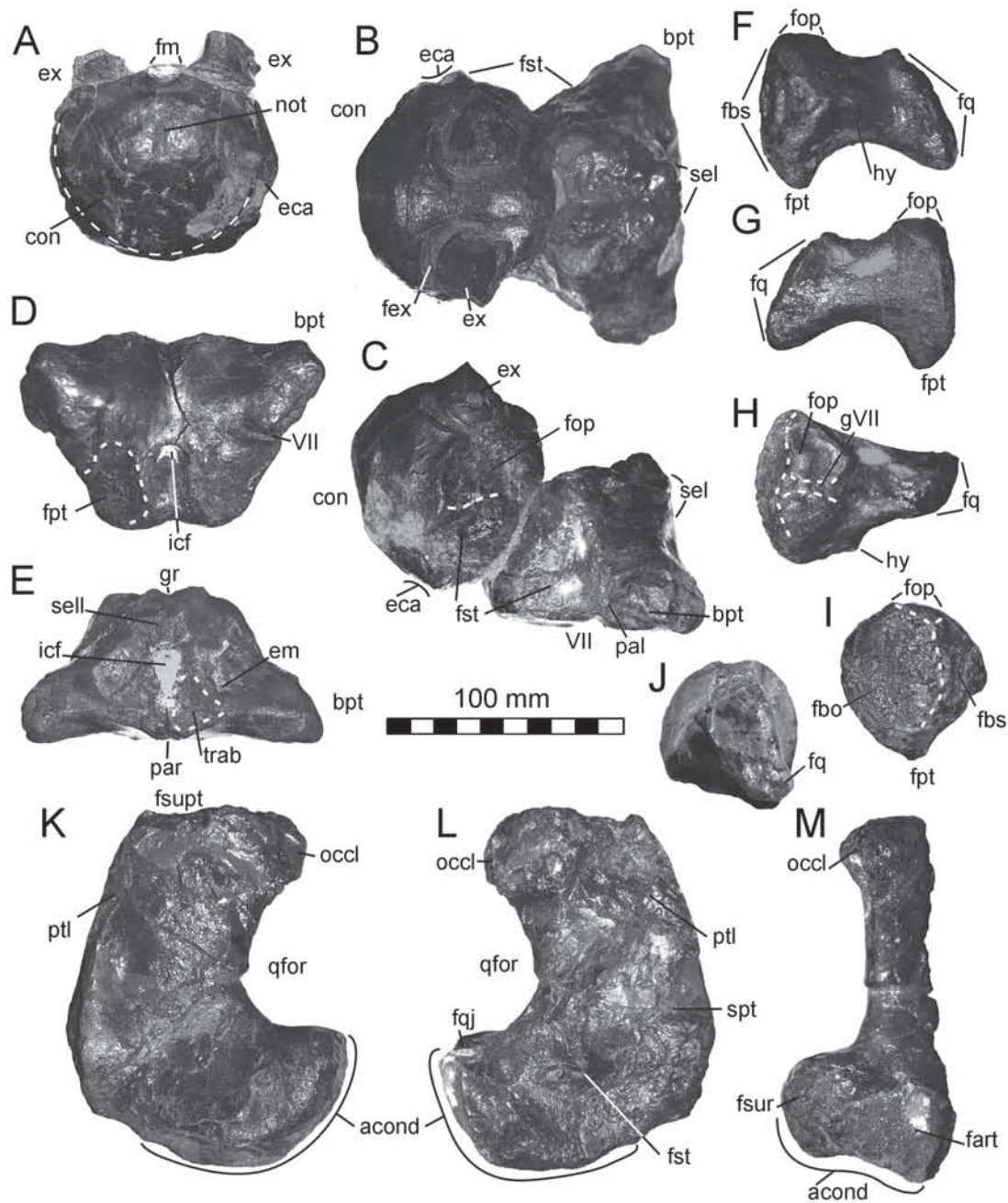


Fig. 3. Basicranium and quadrate of *Grendelius alekseevi* YKM 56702: A – basioccipital and exoccipitals in posterior view; B, C – basioccipital, basisphenoid and exoccipitals in dorsal (B), right lateral (C) views; D, E – basisphenoid in ventral (D), anterior (E) views; F–J – right stapes in posterior (F), anterior (G), dorsal (H), medial (I) views, stapedial lateral facet (J); K–L – left quadrate in lateral (K), medial (L) and posterior (M) views. Abbreviations: acond – articular condyle; bpt – basiptyergoid process; con – condylar surface; eca – extracondylar area; em – pit for origin of eye muscle; ex – exoccipital; fart – condyle boss articulating with articular; fex – facet for exoccipitals; fm – foramen magnum; fbo – facet for basioccipital; fbs – facet for basisphenoid; fop – facet for opisthotic; fpt – facet for pterygoid; fq – facet for quadrate; fst – facet for stapes; fsupt – surface for the articulation with supratemporal; fsur – condyle boss articulating with surangular; gVII – groove for hyomandibular branch of facial (VII) nerve or glossopharyngeal (IX) nerve; gr – median groove; hy – hyoid process; icf – foramen for internal carotid artery; not – notochordal pit; occl – occipital lamella; pal – groove for palatal ramus of facial nerve; par – preserved part of parasphenoid; pti – pterygoid lamella; sel – sella turcica; trab – impressions of trabecular cartilages; spt – surface for articulation with pterygoid; qfor – quadrate foramen; VII – groove for the passage of the palatine ramus of the facial (VII) nerve.

processes are elongated and directed anterolaterally (Fig. 3B, D, E). The basiptyergoid processes are separated posteriorly from the stapedial facet by a broad notch, which encloses a channel for the branch of the facialis (VII) nerve (according to Kirton [1983]; Fig. 3C, D). Posterior to the basiptyergoid processes on the lateral surfaces of the basisphenoid there are large triangle stapedial facets (Fig. 3C). The anterior surface of the basisphenoid is bordered posteriorly by high vertical wall of the dorsum sellae. In the middle part, it is pierced by a large rounded foramen for the internal carotid artery. The remaining place above the anterior carotid foramen is occupied by a short, broad depression, representing the sella turcica. Ventrolaterally to the carotid foramen, there are triangle depressions, probably, accommodating the posterior base of the trabecular cartilage. Small depressions located dorsolateral to the impressions of trabecular cartilages, probably, provided points of attachment for the eye musculature (Fig. 3E). The ventral surface of the basisphenoid is pentagonal in outlines. It bears oval facets for contact with the medial wings of the quadrate rami of the pterygoids (Fig. 3D). The broad basisphenoid-parasphenoid suture is not visible. The foramen for the internal carotid artery is located between the pterygoid facets and continues to the posterior part of the surface as a groove.

The *stapes* (Fig. 3F–J) is robust paired bone consisting of a large head, which articulates with the braincase, and a thick shaft extends ventrolaterally to contact the quadrate. The medial head of the stapes is circular in outline. It bears two facets separated from each other by a low vertical ridge (Fig. 3I). The basisphenoid facet is large and semi-circular in outline. The basioccipital facet is triangular in outline (Fig. 3F, I). Dorsally, both the basisphenoid and basioccipital facets contacts the third elongate triangular facet for the opisthotic (Fig. 3H). This facet is subdivided by a shallow groove, which is commonly interpreted as channel either for the hyomandibular branch of the facialis (VII), or for the glossopharyngeal (IX) nerve (Kirton 1983; Kear 2005). The ventral surface of the stapes forms prominent process for the contact with the medial lamella of the pterygoid (Fig. 3F, G, I). The hyoid process is large (Fig. 3F, H). The stapedial shaft is thick with its distal extremity twisted dorsally approximately 30° relative to the head (Fig. 3F–H). The anterolateral surface of the stapedial shaft is deeply pitted and elongated-oval in outline (Fig. 3J).

The *exoccipitals* (Fig. 3A–C) preserved in natural articulation with the basioccipital. The right one is better preserved. In posterior view, the exoccipital is wide and squat, and its medial and lateral borders are concave (Fig. 3A). The dorsal surface of the exoccipital is slightly convex and bears teardrop-shape facet for the supraoccipital (Fig. 3B). The anterior process at the base of the exoccipital is strongly reduced. The hypoglossal foramina are not observable. Probably XII nerve was excluded from the exoccipital (Fig. 3C).

The *mandible* is presented by three fragments of the left ramus. The posterior part of the ramus is 118 mm in height, and, probably, has been located under the naris and eye. It is formed by the articulated fragments of the most posterior part of the dentary and anterior parts of the angular and surangular (Fig. 2C, D). On the lateral side of the other two fragments belonging to the dentary the deep and narrow fossa dentalis turning into a series of perforations in the most rostral part of the dentary is clearly seen.

Dentition (Fig. 4). Ten teeth anchored in the dental groove of the maxilla. They are damaged in varying degrees; two of them are the young replacement teeth and located in the resorption pits at the bases of the mature teeth (Fig. 4B, C). Teeth are strong.

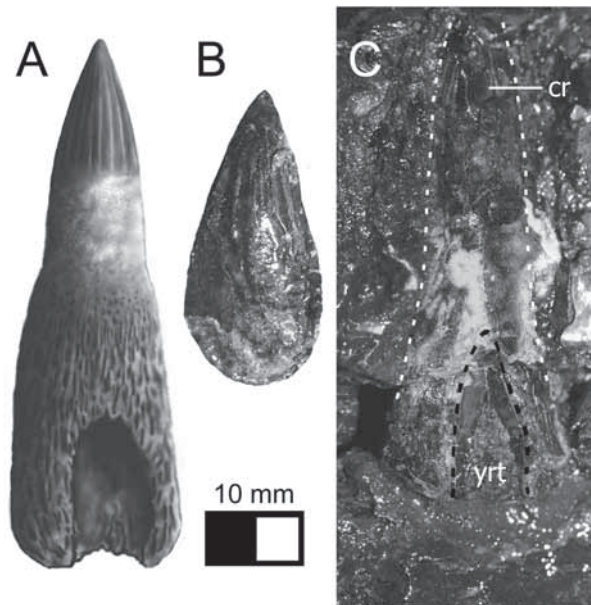


Fig. 4. Teeth of *Grendelius alekseevi* YKM 56702: A – reconstruction; B – crone of young replacement tooth; C – section of a tooth with young replacement one, located in the resorption pit. Abbreviations: cr – crown; yrt – young replacement tooth.



Fig. 5. Atlas-axis complex of *Grendelius alekseevi* YKM 56702 in anterior (A), right lateral (B) and posterior (C) views. Abbreviations: d – diapophysis; fna – facet for neural arch; par – parapophysis.

The conical crowns bear prominent apicobasal ridges, which are located at a considerable distance from each other. Below the crowns, there are smooth inset rings of acellular cementum. The roots are quadrangular in cross-section, slightly swollen and expanding downwards.

Axial skeleton. Centra. A series of 59 vertebrae is preserved; a large part of the presacral vertebrae are in a natural articulation. The vertebral column is poorly regionalized, posterior dorsal-anterior caudal centra ratio is less than 3.5 (criteria according to Maxwell [2010]).

The atlas and axis are fused without any visible suture; they are slightly narrowed ventrally (Fig. 5A, B). The ventral surface of the atlas-axis complex is rounded. The anterior surface of the atlas is less concave than the posterior surface of the axis. The facet for atlantal intercentrum is slightly prominent and shifted ventrally (Fig. 5A). The torus-like diapophyses are confluent with the facets of the neural arches, directed obliquely anteroventrally. The parapophyses are rounded in outline; their articular surfaces are excavated. On the axis, they are located right on the posterior edge of the bone.

The anterior presacral centra are rounded in cross-section. Here the parapophyses have a rounded shape; the diapophyses are confluent with the facets for the neural arches. The diapophyses begin to separate from the neural arches in the 25th vertebra and abruptly descend in the ventral direction. They have shifted halfway down at the 33rd centrum.

The posterior dorsal vertebrae are narrowed dorsally; therefore, they have a pear-like outline in anterior view. Shape of the anterior caudal centra is also pear-like, becoming rounded at the posterior caudal centra.

Neural arches (Fig. 6). The neural arches are preserved in the articulation with most of the presacral vertebrae. There are several caudal neural arches, which were separated from the centra in situ due to taphonomical conditions (Arkhangelsky et al. 2000). In total, there are 45 neural arches. The neural spines quickly reach a maximum height exceeding the height of the centra in 1.3 times. Gradual decrease in height, along with the increase of the angle of posterior inclination of the spines begins from near the 23rd vertebra. The anterior spines are more slender than posterior, which is a characteristic feature of ichthyosaurs (McGowan and Motani 2003). The anterior presacral neural arches are characterized by the vertically directed (parallel to the centra) spines, wherein the angle of the spine with the anterior zygapophysal surface is 135–140° (Fig. 6). This angle increases in the more caudally located arches until reaching approximately 180° at the 28th vertebra. Here the adjacent dorsal ends of the spines are oriented in a way that the anterior angle of each of the spine is located higher than the posterior angle of the previous.

The pedicles of the neural arches are low. Ventrally they expand in the anteroposterior direction.

The dorsal surfaces of the presacral spines are concave and tuberous for the application of a car-



Fig. 6. Neural arches of *Grendelius alekseevi* YKM 56702. Abbreviations: az – anterior zygapophysis; cp – columnar pedicles; ns – neural spine; pz – posterior zygapophysis.

tilaginous cap (Fig. 6). The dorsal surfaces of the caudal spines are rounded and ossified.

Ribs. Fifty-six ribs of varying preservation are presented in YKM 56702, mainly relating to the left side of the trunk. The length of the best-preserved and longest one is 700 mm. The furrows extend from the capitulum and the tuberculum in ventral direction giving the rib 8-shaped cross-section in proximal two-thirds of its length; distally the rib is oval in cross-section. The articulated surfaces of the capitulum and tuberculum in the anterior trunk ribs are convex; they divided by the shallow notch. The articulated surfaces of the heads of the posterior dorsal ribs are flat; the tuberculum extends far medially than the capitulum, the notch between them becomes deeper.

Pectoral girdle (Fig. 7). The bones of the pectoral girdle are completely preserved. **Coracoid** (Fig. 7K–N). The coracoid is robust, roughly circular, with a prominent anterior notch (Fig. 7L, N). Its dorsal and ventral surfaces are saddle-shaped. The medial articular surface is lenticular in medial view (Fig. 7M). In situ the bones were in a natural articulation (Arkhangelsky et al. 2000). The glenoid and the scapular facets are facing anterolaterally and forming an angle about 165°. The scapular facet is deeply pitted triangle in outline, which is not markedly separated from the large, lenticular glenoid contribution. The anterior notch is relatively narrow and deep. The anterior process of the coracoid is well developed. The posterior border of the coracoid is strongly flattened, gradually curving dorsally.

Scapula (Fig. 7A–F). The scapular shaft is thick and rod-like. It slightly arcuately curves in dorso-posterior direction (Fig. 7A–E). The shaft is subtriangular in cross-section at its midpoint, but becomes more oval distally and finally flattens immediately in the markedly anteroposteriorly expanded dorsal end (Fig. 7B). The scapular dorsal border is rugose indicating presence of an unossified cartilaginous elongation in vivo. The ventral margin of the scapula gradually expands anteroposteriorly. A large acromial process curves ventrally giving to the ventral margin of the scapula an ‘S’-shaped form (Fig. 7A–G). The coracoid facet is triangular and continuous with subequal in length glenoid contribution (Fig. 7F, G).

Clavicle. The clavicle is robust. Its medial end is broad and flattened, lateral parts are smoothly bended posterodorsally. Its pointed end is circular in cross-section, being over a third of the length of the clavicle it gently articulates with the anterior border of the scapula. Right clavicle in its middle part bears a lump-like nodosity – trace of an in vivo healed fracture (Arkhangelsky 2001; Stepanov et al. 2004).

Interclavicle (Fig. 7H, I, J). The interclavicle is robust element. The anterior transverse bar of the interclavicle is convex, with a low wall, its lateral extremities extend posterodorsally and sharpened. The ventral and anterior surfaces are divided by the shaft, which forms in the middle a slightly pointed knob with posteriorly directed bur (Fig. 7I). The posterior median stem of the interclavicle is strongly shortened, flattened and expanded, its posterior edge is rounded (Fig. 7).

Forefins (Fig 8). The both forelimbs are preserved articulated in situ. During excavation, the elements were plotted on tracing paper and numbered (Arkhangelsky et al. 2000).

Humerus (Fig. 9). The proximal end of the humerus is strongly expanded and its distal end is flattened. Proximal end is roughly trapezoidal in cross-section; its surface is slightly convex and nodular (Fig 9D). Humeral torsion is absent. The prominent plate-like dorsal process extends obliquely forward towards the front edge of radial facet up to the level of diaphysis (Fig. 9A, C). The robust and triangle deltopectoral crest is located in ventral surface (Fig. 9A). The posterior edge of the humerus is blade-like flattened along the entire length. This condition causes keel-like protrusion of the posterior edge of the proximal part of the humerus (Fig 9B, D). The distal end of the humerus bears four facets: for radius, intermedium,

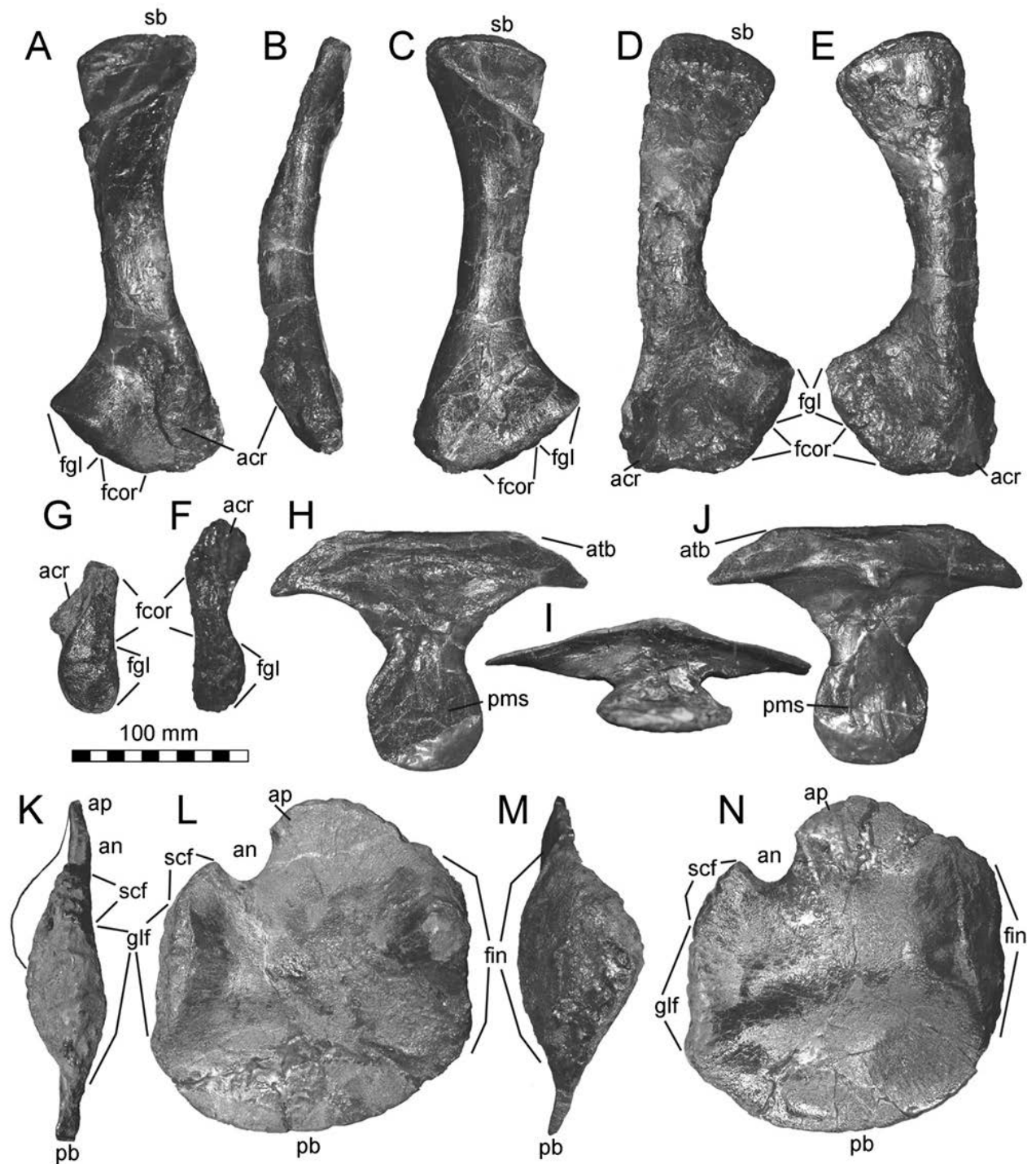


Fig. 7. Pectoral girdle of *Grendelius alekseevi* YKM 56702. A–C, G – right scapula in lateroventral (A), anterior (B), dorsomedial (C) views and its medial surface (G); D–F – left scapula in lateroventral (D) and dorsomedial (E) views and its medial surface (F); H, I, J – interclavicle in dorsal (H) posteroventral (I) and ventral (J) views; K – lateral surface of left coracoid; L – right coracoid in ventral view; M – left coracoid in medial view; N – left coracoid in dorsal view. Abbreviations: acr – acromion process; an – anterior notch; ap – antero-medial process; atb – anterior transverse bar; fgl – glenoid contribution of the scapula; fcor – coracoid facet; fin – intercoracoidal facet; glf – glenoid contribution of the coracoid; pb – posterior border; pms posterior median stem; sb – scapular dorsal border; scf – scapular facet.

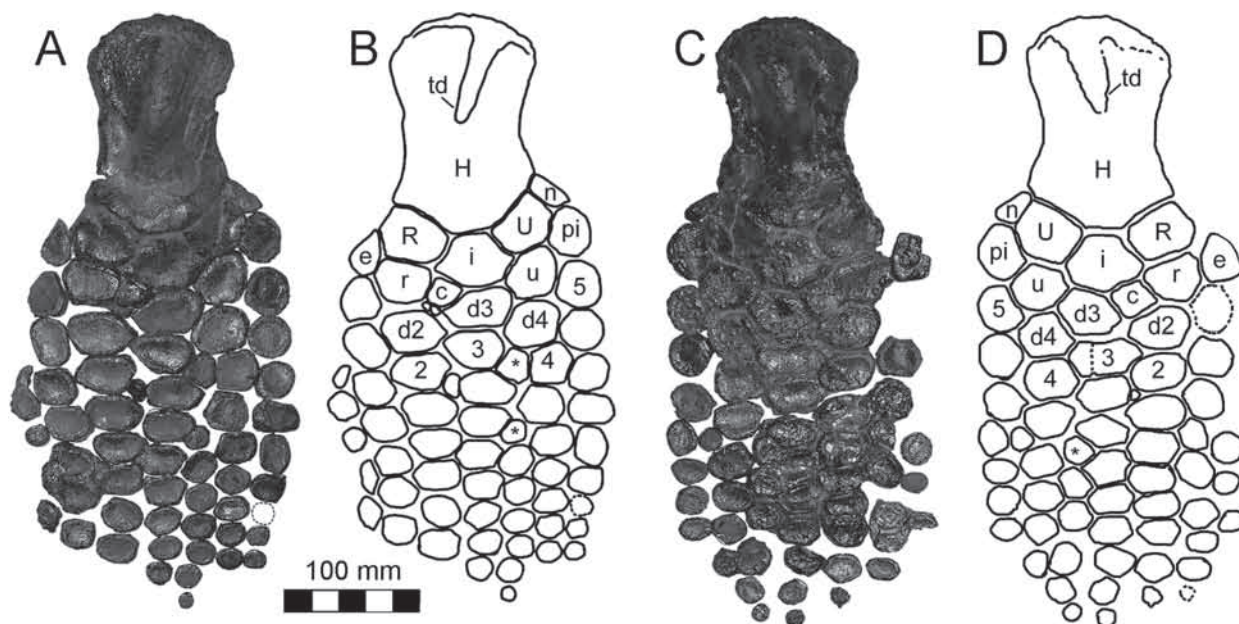


Fig. 8. Forefins of *Grendelius alekseevi* YKM 56702. Photograph and interpretive outline of the left (A, B) and right (C, D) forefins in dorsal view. Abbreviations: 2–5 – metacarpals; d2–d4 – distal carpals 2–4; c – neomorphic ossicles convergent to centralia; e – first element of the anterior accessory digit; H – humerus; i – intermedium; n – neomorph; pi – pisiform; R – radius; r – radiale; td – trochanter dorsalis; U – ulna; u – ulnare; * – interstitial digit.

ulna and posterior neomorph. The angle between radial and intermedial facets is 130° , between intermedial and ulnar facets – 135° . Thus, radial facet is facing anterodistally and ulnar facet facing posterodistally (Figs. 8, 9A).

Epipodium (Figs. 8, 9A–C). The epipodium is composed of four elements: radius, ulna, intermedium and posterior neomorphic ossicle.

The *radius* is roughly pentagonal in outlines, tapering anteriorly and forming a keel. Anterodistally it contacts with the first element of the anterior accessory digit, distally with the radiale, medially with the intermedium.

The *ulna* is isometric and pentagonal in outline. Medially it contacts with the intermedium, distally – with the ulnare, posterodistally with the pisiform, posterally with the posterior neomorph.

The *intermedium* is approximately hexagonal in outline. Proximally, it contacts the humerus, anteroproximally, the radius, posteroproximally, the ulna. Anterodistally, the intermedium possess small contact with the radiale and derivates the neomorphic elements convergent to centralia (see remarks). Distally, the intermedium contacts the distal carpal three, and posterodistally – ulnare.

The radius, ulna and intermedium have approximately the same size. They rapidly narrow distally so that their proximal surfaces are twice wider than the distal ones.

The *posterior neomorph* is isosceles trapezoid in outline. It is strongly flattened and its posterior edge continues sharpened posterior edge of the humerus. The bone bears three facets: triangular distal facet for the pisiform, rectangular anterodistal for the ulna and anteroproximal for the humerus.

Autopodium (Fig. 8). The radiale bears the following facets: the anterodistal facet for the first phalanx of the preaxial accessory digit, distal facet for the distal carpal 2, anteroproximal facet for the first element of the preaxial accessory digit, posterior facet for the neomorphic element and intermedium. The ulnare bears the following facets. The anterodistal facet for the distal carpal 3, proximal facet for the ulna, posteroproximal facet for the pisiform, anteroproximal facet for the intermedium, posterodistal facet for the metacarpal 5, distal facet for the distal carpal 4.

The epipodial and autopodial elements are polygonal with rounded corners; most distal elements are rounded indicating a large amount of cartilage in the space between them. The epipodial to autopodial

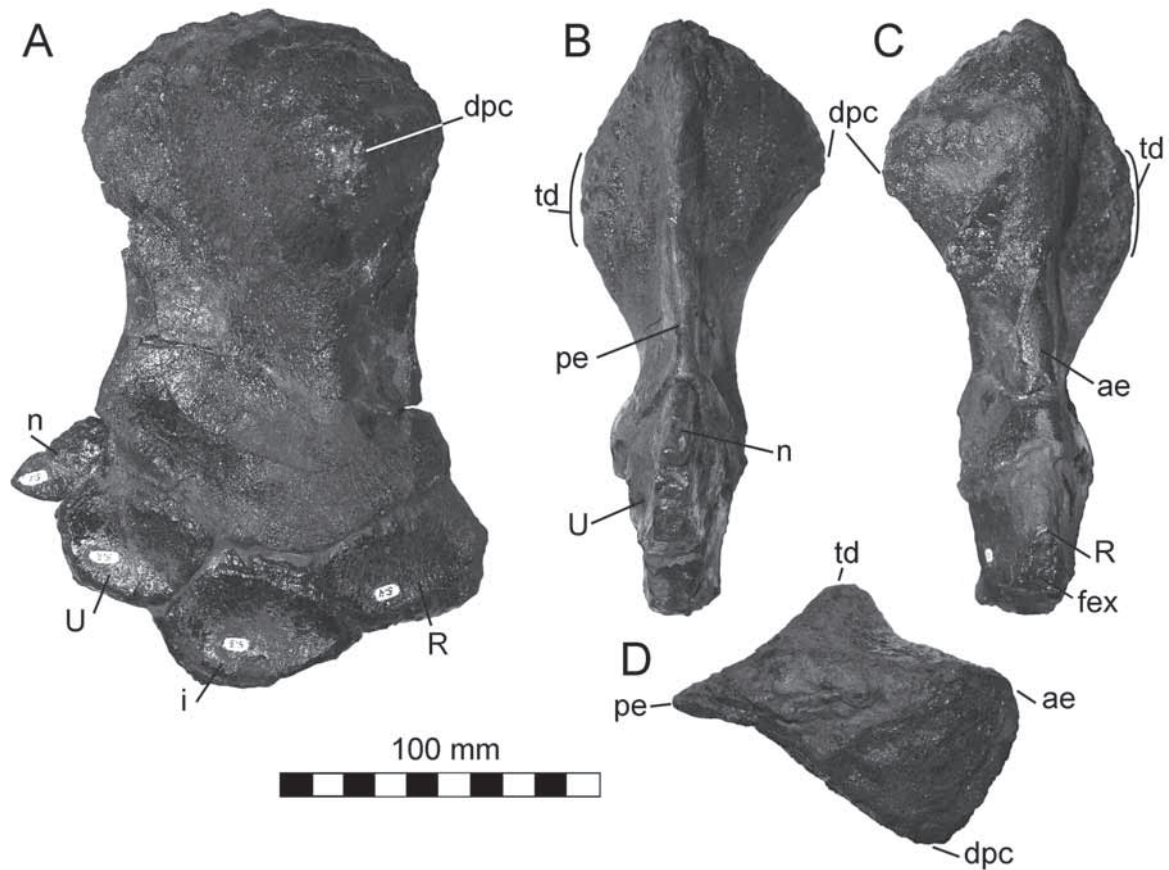


Fig. 9. Right humerus and epipodium of *Grendelius alekseevi* YKM 56702 in ventral (A), posterior (B), anterior (C) and proximal (D) views. Abbreviations: ae – anterior edge; dpc – deltopectoral crest; pe – posterior edge. For other abbreviations, see Fig. 8.

elements are flattened and plate-like. Their thickness does not exceed 8 mm.

The digits are short; the greatest number of phalanges is eight. There are two preaxial accessory digits. The digit 3 is bifurcating at the level of the phalanx 3, additional ossification presents at the level of its metacarpal and the phalanx 1.

Comparison. Being a basal platypterygiine, *Grendelius alekseevi* shares a number of common ophthalmosaurine features. The ‘C’-shaped quadrate, having markedly expanded dorsal and ventral extremities, resembles the one of ophthalmosaurine ichthyosaurs and *Sveltonectes insolitus* (Andrews 1910; Kirton 1983; Fischer et al. 2011, 2012). The anterior process at the base of the exoccipital is strongly reduced as in *Sveltonectes insolitus* (Fischer et al. 2011). The rounded ventral surface of the atlas-axis complex differs from those of derived platypterygiines (Broili 1907; Wade 1990; Maxwell and Kear 2010), in which

it is laterally limited by the depressions. The condition of the anterior surface of the atlas less concave than the posterior surface of the axis is unusual for ichthyosaurs (McGowan and Motani 2003); this condition could cause the restriction of head movements. The diapophyses separation from the neural arches in the 25th vertebra and shift halfway down at the 33rd centrum is a condition consistent with *Ophthalmosaurus* (Kirton, 1983). In general outline the coracoid of *G. alekseevi* is similar to that of *Undorosaurus* (Efimov 1999b), having the posterior part mediolaterally longer than the anterior part. Its dorsal and ventral surfaces are saddle-shaped as in some ophthalmosaurine ichthyosaurs (Andrews 1910; Fischer et al. 2012). Relatively narrow and deep anterior notch of the coracoid is similar to that of *Sveltonectes* (Fischer et al. 2011). The medial portion of the scapula is less expanded than in *G. pseudoscythicus* (Efimov 1998). The thick and rod-like

scapular shaft was also described for *P. hercynicus* (Kolb and Sander, 2009).

Grendelius alekseevi differs from the congeners by flattened humerus with diminished torsion, presence of two preaxial accessory digits, neomorphic centralia and additional neomorphic postaxial ossicle contacting the humerus. The deltopectoral crest is similar to that of *Ophthalmosaurus* (Andrews 1910; McGowan and Motani 2003). It is not flattened like in platypterygiines (McGowan and Motani 2003; Fischer et al. 2014a).

The flattened epipodial to autopodial elements is typical condition for the Early Jurassic forms e.g. *Temnodontosaurus*, *Stenopterygius* (Maisch and Matzke 2000) and uncommon for Ophthalmosauridae (Fischer et al. 2011). In *G. alekseevi*, autopodial elements has probably thinned repeatedly and independently as an autapomorphy.

Remarks. Both forefins of YKM 56702 possess neomorphic ossicles, located anterodistally to the intermedium. In the reptilian forelimb, the intermedium bifurcates to form the condensations of the centralia 2 and 3, according to the provisions of limb patterning as a hierarchical sequence of “branching” events (Shubin and Alberch 1986). Thus, it is most likely that neomorphic ossicles observed in YKM 56702 are convergent to the centralia. In that case, it is the first record of the centralia in Ophthalmosauridae. However, centralia were reported for basal Ichthyosauromorpha Motani et al., 2014 – hupesuchians (Carroll and Dong 1991; Chen et al. 2014) and *Chaohusaurus* Young et Dong, 1972 (Motani et al., 2015).

Unfortunately, at the present time, some parts of the skeleton: clavicles, ribs, part of the caudal vertebrae and some fragments of the skull (incomplete jugals and postorbitals, strongly deformed fragments of the skull roof, supraoccipital, fragments of the lower and upper jaws, noted by Arkhangelsky (2001), are on the restoration, on account of progressive pyrite decay. Therefore, they could not be photographed. Traces of pyrite decay begin to appear on the examined material, they can be seen on some figures as a white plaque, thus it is also necessary to carry out the restoration of these bones in the near future.

***Grendelius zhuravlevi* (Arkhangelsky, 1998),
comb. nov.**

Brachypterygius zhuravlevi: Arkhangelsky, 1998: 90, fig. 4.
Otschevia zhuravlevi: Pervushov et al., 1999: 27; Arkhangelsky, 2000: 79, figs. 1, 2; 2008: 252, fig. 6.

Brachypterygius pseudoscythius: Maisch and Matzke, 2000: 79; Maisch, 2010: 167.

Brachypterygius extremus: McGowan and Motani, 2003: 117.

Holotype. PIN 426/60–76 left humerus with the elements of the epipodium and autopodium; Saratov Province, Krasnopartizansky District, Gornyi settlement, Savelevskii Shale Mine; Upper Jurassic, Middle Volgian, Dorsoplanites panderi zone.

Referred specimen. SRM Hb 30192, mounted skeleton: fragmentary lower jaw, incomplete vertebral column, fragmentary ribs, humerus, elements of epipodium and autopodium, left femur; Russia, Samara Province, Syzran District, Kashpirskoe Pyroshale Field (Mine № 3); Upper Jurassic, Middle Volgian substage, lower part of Dorsoplanites panderi zone.

Diagnosis. Modified from Arkhangelsky (1998, 2000). Changes listed below: a medium-sized platypterygiine ichthyosaurs, characterized by the following unique combination of features: posterior edge of the humerus is machete-like in outline, being strongly flattened all along its length; autopodial elements are thick and brick-like; ulna is trapezoid in outline, bearing a facet for the pisiform all along the posterior edge; prominent muscular tubercle on dorsal border of the ulnar facet of the humerus.

Description. Measurements of SRM Hb 30192 are given in Table 2.

Skull. Several cranial fragments are preserved including fragmentary nasal, surangular and dentary, which allow providing the following observations. The tapering anterior extremities of the nasal run concealed beneath the premaxilla anteriorly for about 20 cm. The low coronoid process is raised on the dorsal edge of preserved part of the surangular.

Axial skeleton. There are 40 vertebral centra in the examined material. The anterior dorsal vertebrae (17 centra preserved) are tapered ventrally and characterized by confluence of the diapophyses with the facets for the neural arches. The diapophyses are semi-rhomboid in outline. The parapophyses are quadrangular and barely separated from the anterior edge of the centrum on the anterior most vertebrae and gradually detached from it in more caudally located trunk centra. The posterior trunk centra (14 centra preserved), compared with preceding are slightly expanded ventrally and tapered dorsally. Their diapophyses are from rectangular to circular in outline, fusing with the anterior border in some centra. The parapophyses are rounded. The rib facets

Table 2. Measurements (mm) of the propodial bones of *Grendelius alekseevi* (YKM 56702), *Grendelius zhuravlevi* (SRM Hb 30192) and *Platypterygiinae* gen. et sp. indet. (SGM 1566).

Bone	Length	Width			Measurements
		proximal end	distal end	diaphysis	
Left humerus YKM 56702	154	104	106	85	radial facet – 47; ulnar facet – 40; facet for intermedium – 30; for neomorph – 10
Right humerus SGM 1566	148	120	100	80	radial facet – 48; ulnar facet – 50; facet for intermedium – 15;
Humerus SRM Hb 30192	124	98	93	63	radial facet – 37; ulnar facet – 40; facet for intermedium – 27
Femur SRM Hb 30192	82	48	56	37	tibial facet – 21; fibular facet – 32

are located below the mid-height on the preserved posterior trunk vertebra. The posterior dorsal – anterior caudal centra are long, indicating poor regionalization of the vertebral column. The anterior caudal centra are pear-shaped in outline tapering dorsally. They bear single rounded rib facets. The posterior caudal vertebrae (four centra preserved) are rounded bearing relatively large squared rib facets on their ventrolateral parts.

Forefins (Fig 10, 17E). *Humerus* (Fig 10A–F). Both the left and right humeri are preserved in SRM Hb 30192. Left humerus is better preserved; in general proportions, it resembles that of the holotype. In proximal view, the humerus has machete-like outline (Fig. 10F). Humeral ‘torsion’ is prominent: the long axes of the proximal and distal ends of the humerus are twisted at an angle of 50° in SRM Hb 30192 (70° in the holotype). Posterior edge of the humerus is strongly flattened all along its length (Fig. 10D). The ventral surface of the humerus is slightly concave all along the bone length (Fig. 10B). The trochanter dorsalis is prominent and plate-like. It extends up to the half of the length of the humerus, from the proximal posterior towards the distal anterior (Fig. 10A). The deltopectoral crest in SRM Hb 30192 is poorly developed, its ventral protrusion is caused by humeral ‘torsion’ (Fig. 10B, C, F); in the holotype the deltopectoral crest is pointed and therefore more prominent. The muscular tubercles are pronounced on the dorsal and ventral surfaces near the ulnar facet in the holotype and only on dorsal surface in SRM Hb 30192 (Fig. 11). The humerus expands distally bearing three deep and rugose distal facets (Fig.

10E). The facets for articulation with the radius and ulna are semicircular in outline; the facet for articulation with the intermedium is parallelogram-shaped. The length of the facet for the intermedium on the humerus of SRM Hb 30192 is relatively increased, compared with the holotype. The radial forms angle 130° with respect to the ulnar facets in SRM Hb 30192 and 103° in the holotype. Thus, the ulnar facet is facing posterodistally and radial facet is facing anterodistally.

Epipodium (Fig. 10G–K). The epipodium is composed of three elements: radius, intermedium and ulna.

The radius is roughly rectangular in outline; it contacts with the basal element of the preaxial accessory digit anterodistally, with the radiale distally and with intermedium posteriorly. The intermedium is hexagonal in outline, it contacts with the radius anteroproximally, with the ulna posteroproximally, with the radiale anterodistally, with the ulnare posterdistally, and bears a flat broad surface for the contact with distal carpal 3 distally. The ulna is trapezoid in outline contacting with the intermedium medially, with the ulnare distally. The posterior edge of the ulna is narrowed; it bears a deep furrow all along its length – facet for the pisiform. The epipodial elements are greatly expanded proximally. Their proximal surfaces are rugose and slightly convex. Epipodial to autopodial elements are strongly thickened.

Autopodium (Fig. 10L–O). Eight autopodial elements are preserved. They are hexagonal and brick-like, with the thickness exceeding their height (Fig. 10N, O). Some of the autopodial elements bear

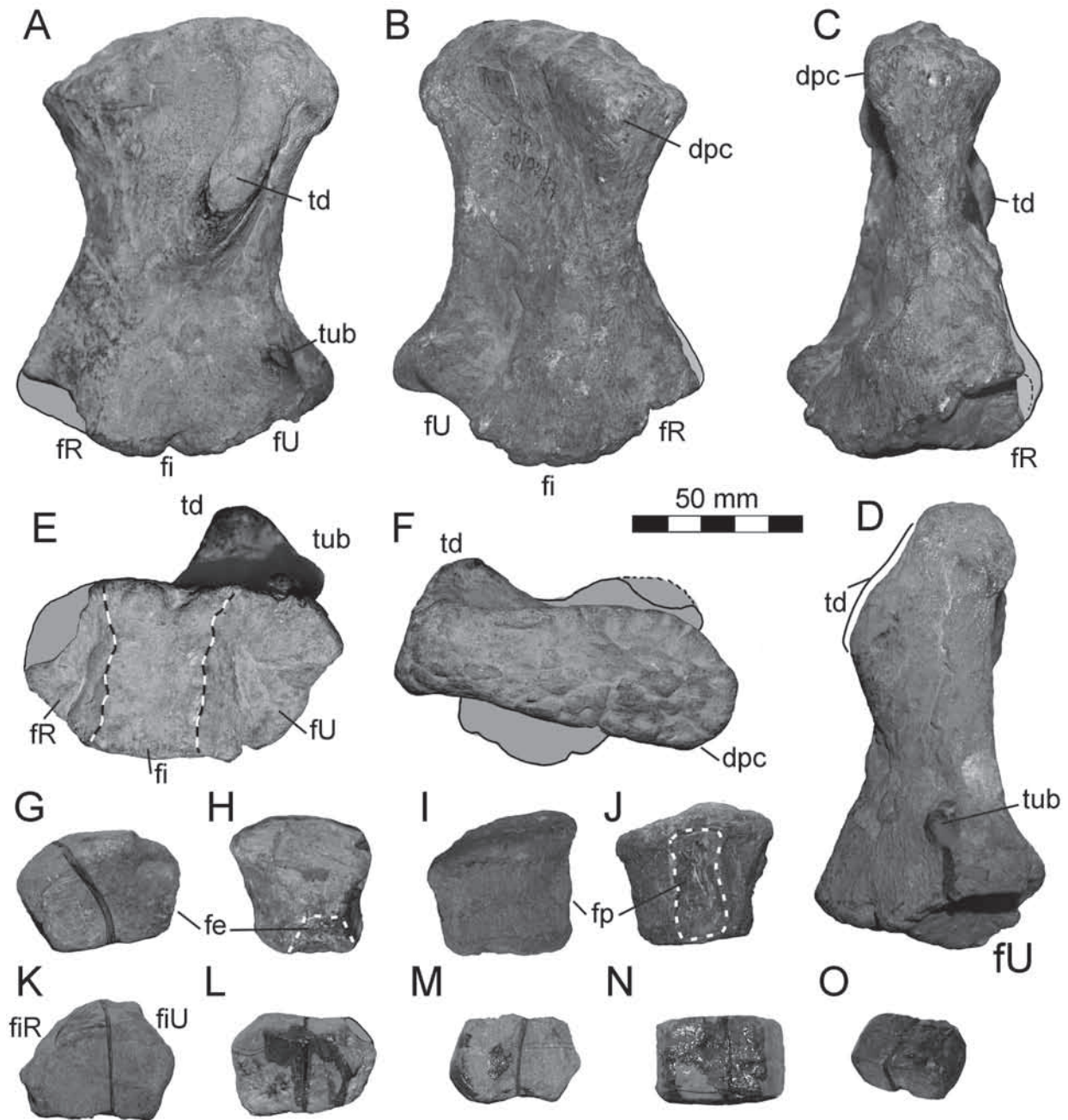


Fig. 10. Elements of the right forelimb of *Grendelius zhuravlevi* SRM Hb 30192: A–F – right humerus in dorsal (A), ventral (B), anterior (C), posterior (D), distal (E) and proximal (F) views; G, H – radius in ventral and anterior views; I, J – ulna in dorsal and posterior views; K – intermedium in dorsal view; L–O – autopodial elements. Abbreviations: fe – facet for the first element of the anterior accessory digit; fi – intermedial facet; fiR – facet of intermedium for radius; fiU – facet of intermedium for ulna; fp – facet for pisiform; fR – radial facet; fU – ulnar facet; for other abbreviations see Figs. 8 and 9.

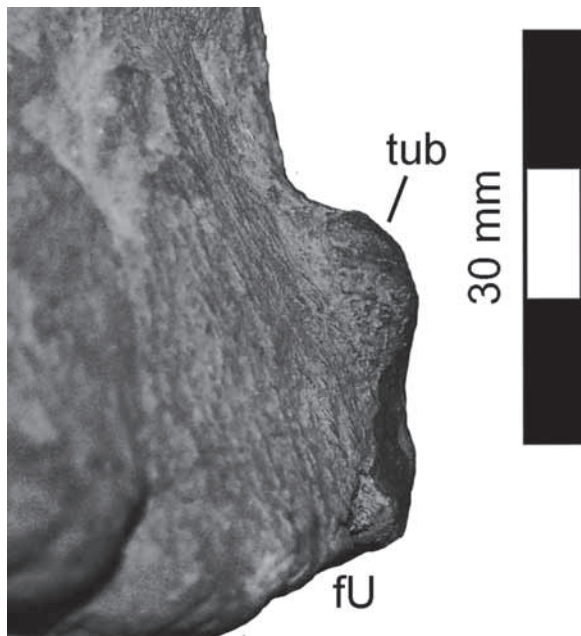


Fig. 11. Muscular tubercle on the dorsal surface of the humerus of *Grendelius zhuravlevi* SRM Hb 30192.

notches on their dorsal and ventral borders (Fig. 10M, O). Two of these elements were identified as the radiale and ulnare.

Femur. We follow the orientation of the femur of ophthalmosaurids proposed by Maxwell et al., (2012). The right femur is preserved. In proximal view, the femur has a triangular outline (Fig. 12F). The prominent ventral process lies close to the anterior edge of the femur, it extends approximately 2/5 of the length of the femur (Fig. 12A, C). The substantial part of its surface is rugose – it was covered by cartilage in vivo. The dorsal process is situated closer to the anterior edge of the femur; it is narrower and less robust than the ventral process (Fig. 12B, C). The anterior surface of the femur is concave proximally. The posterior surface is convex all along its length, forming the posterior keel (Fig. 12D). The two distal facets are markedly concave. The anterior distal facet for articulation with the tibia is twice smaller than the posterior fibular facet. The tibial facet forms a more acute angle with respect to the long axis of the femur, than does the fibular facet.

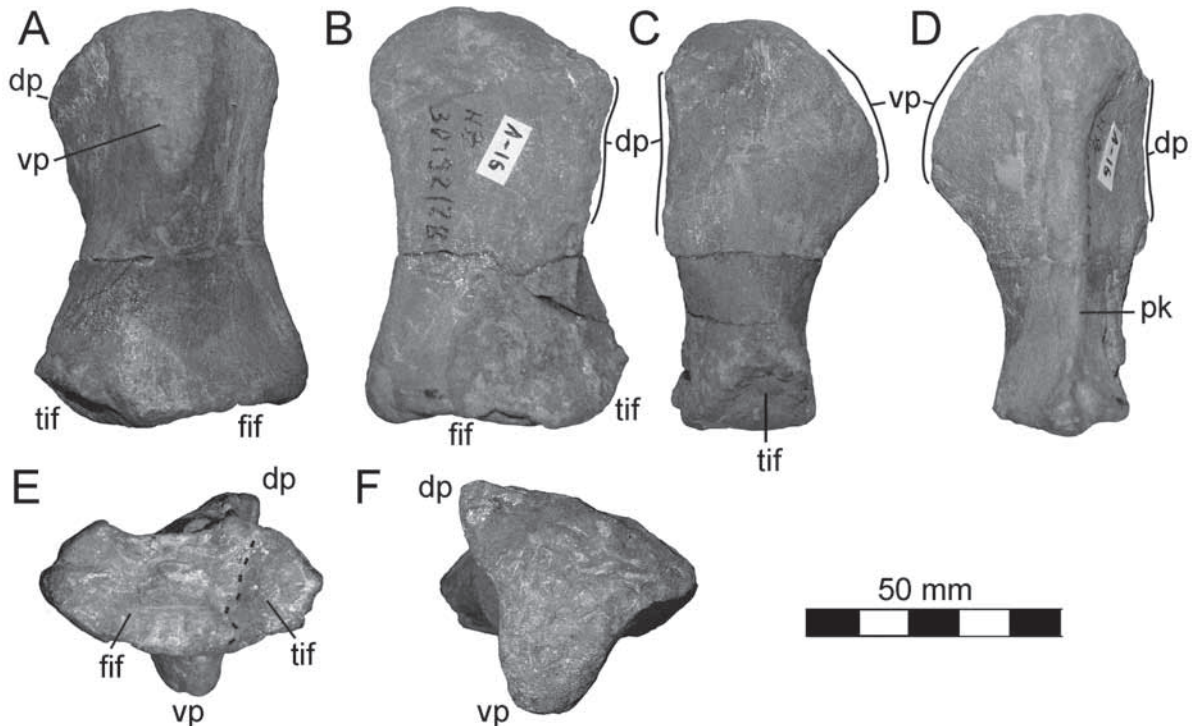


Fig. 12. Right femur of *Grendelius zhuravlevi* SRM Hb 30192 in ventral (A), dorsal (B), anterior (C), posterior (D), distal (E) and proximal (F) views. Abbreviations: dp – dorsal process; fif – fibular facet; pk – posterior keel; tif – tibial facet; vp – ventral process.

Comparison. The main difference of *Grendelius zhuravlevi* from its congeners is strongly dorsoventrally flattened proximal end of the humerus and prominent humeral torsion (similarity with *Brachypterygius*). The trapezoidal outline of the ulna (pentagonal in all other ophthalmosaurids) is also unique for this species. The ulna is trapezoidal due to long posterior facet for the pisiform, faced posterodistally in other *Grendelius* species. Tightly packed rectangular phalanges with dorsal and ventral notches are similar to *Brachypterygius* and derived platypterygiines (Kirton 1983; Maxwell and Kear 2010). The configuration of the distal facets of the femur in *Grendelius zhuravlevi* is uncommon for ichthyosaurs: the tibial facet forms a more acute angle with respect to the long axis of the femur, than the fibular facet. In Ichthyosauria, tibial facet usually exceeds in size the fibular facet and forms a right angle in respect to the long axis of the femur (Maxwell et al. 2012).

Remarks. The basioccipital mentioned in the material by Arkhangelsky (2000) is now absent. Several autopodial elements are also gone.

Platypterygiinae gen. et sp. indet.

Material – SGM 1445–1, the atlas-axis complex and four presacral centra, right coracoid and partial right forefin; unknown locality, Middle Volgian (probably *Dorsoplanites panderi* zone), according to micropaleontological analyzes of the matrix.

Description. Measurements of SGM 1445–1 and SGM 1566 are given in Table 3.

Axial skeleton. The atlas and axis are fused with a prominent ventral scar, forming a ventral protrusion (Fig. 13B). The vertebrae are tapered ventrally. The

Table 3. Measurements (mm) of Platypterygiinae gen. et sp. indet. SGM 1445–01 and SGM 1566.

Bone	Length	Width	Height	Additional measurements
atlas-axis	65	105	90	–
coracoid	–	175	medial facet – 70	scf – 40; glf – 100

facet for the atlantal intercentrum is broad and low, shifted to the ventral edge of the centrum. The ventral keel is poorly prominent on the ventral surface of the atlas originating on the axis. The atlas bears a flat tuberosus anterior articular surface for the basioccipital radically different from a deeply concave posterior surface of the axis. The diapophyses and parapophyses on the atlas are completely fused together and with the facet for the atlantal neural arch forming a broad bumpy surface with sinusoidally curving posterior. The facets for the neural arches on the atlas are turned slightly anteriorly and deep. The axial diapophyses are confluent with the facets of the neural arches and posterior borders of the atlantal diapophyses. They are elliptical in outlines and directed anteroventrally. The axial parapophyses are rounded, locating in the middle of the central length, and not fusing its posterior edge. On the right side of the axis, two facets similar in size and shape are present. One of them is parapophysis and the second is of unclear function, and can be interpreted as an anomaly.

The first four anterior dorsal vertebrae have different degrees of preservation. The third vertebra is better preserved. It is cordate-shaped. The diapophyses are wide and confluent with the facets for the

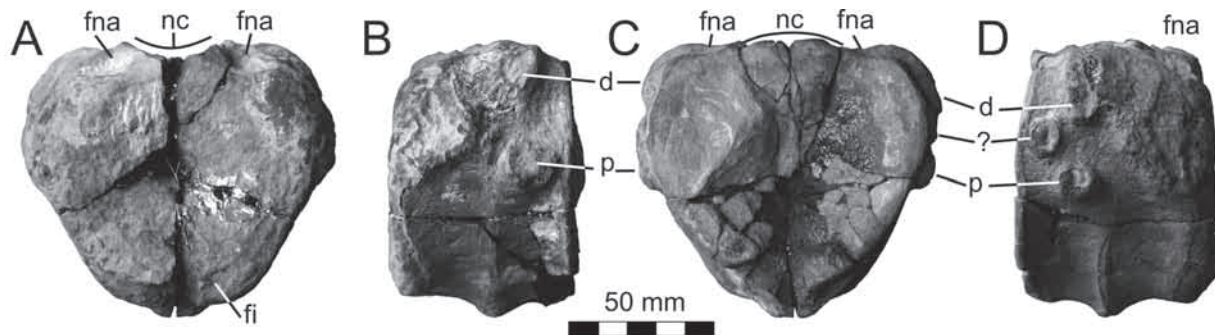


Fig. 13. Atlas-axis complex of SGM 1445–1 in anterior (A), left lateral (B), posterior (C) and right lateral (D) views. Abbreviations: d – diapophysis; fi – facet for atlantal intercentrum; fna – facet for neural arch; nc – floor of neural canal; par – parapophysis; ? – indeterminate rib facet.

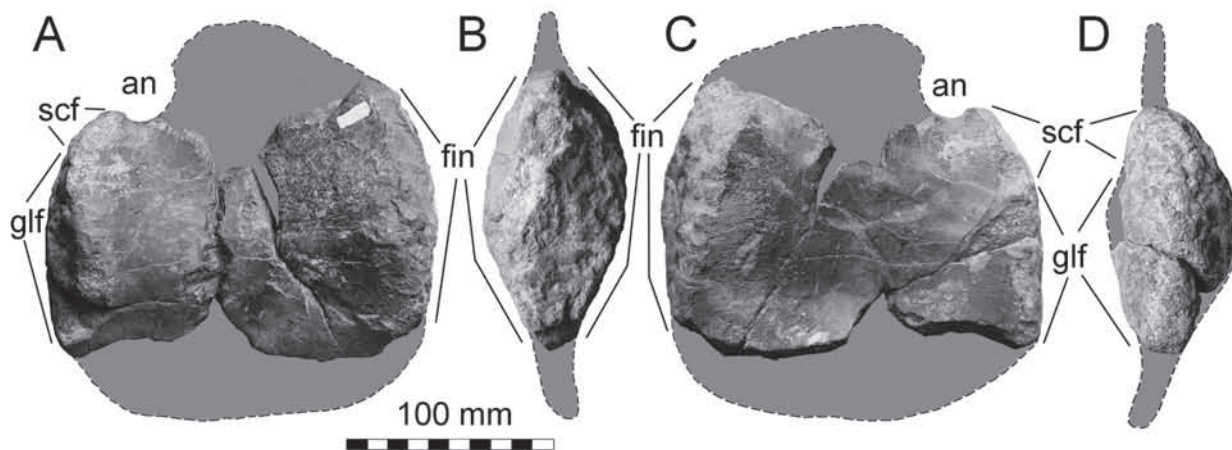


Fig. 14. Right coracoid of SGM 1566 in ventral (A); medial (B); dorsal (C) and lateral (D) views. For abbreviations see Fig. 7.

neural arch and anterior edge of the centrum. The parapophyses are rounded and located closer to the anterior edge of the centrum.

Coracoid (Fig. 14). The pectoral girdle is represented by the right coracoid with broken anterior process and posterior border. The anterior notch is narrow. The medial articular surface is lenticular in medial view (Fig. 14B). The dorsal surface of the bone is saddle-shaped; the ventral surface is relatively flat (Fig. 14A, C). The preserved part of the posterior border is curving dorsally (Fig. 14C). The glenoid and the scapular facets are broad facing anterolaterally and forming angle about 150° . They are deeply pitted and poorly separated from each other. The scapular facet is triangular in outline, the glenoid contribution is lenticular and swollen (Fig. 14D).

Forefin. Humerus (Fig. 15A–F). The preserved right humerus is partially broken. The posterior edge of the humerus is slightly tapered all along its length (Fig. 15C). The proximal end is semi-oval in outlines due to the wide and strongly developed trochanter dorsalis and deltopectoral crest (Fig. 15E). The prominent humeral ‘torsion’ is present: the long axes of the proximal and distal ends of the humerus are twisted at an angle of 70° . The humeral torsion is caused by dorsoventral prolongation of the development of both dorsal process and deltopectoral crest. The dorsal process is robust, plate-like, extending up to the half of the length of the humerus (Fig. 15A, C). The deltopectoral crest is large and strongly developed (Fig. 15B, D). There are three distal facets. The facets are semi-circular, faced anterodistally and posterodistally for the radius and ulna respectively.

The narrowest facet, located between them, is for the contact with the intermedium (Fig. 15F). The angle between the radial and ulnar facets is 115° .

Epipodium and autopodium (Fig. 15G–O). The radius, ulna and six autopodial elements are preserved. The radius is semi-pentagonal in outline, with distal facet for the radiale, anterodistal facet for the first element of the anterior additional digit and posterior facet for the intermedium (Fig. 15H). Its proximal surface for the articulation with the humerus is flat. The ulna is posteriorly broken (Fig. 15G). Its preserved anterior part suggests that it was longer than the radius. The proximal autopodial elements are thickened and brick-like with slightly rounded corners (Fig. 15I–M). The most distal autopodial elements are rounded in outline (Fig. 15N, O).

Comparison. The above-described remains could be identified only as *Platypterygiinae* gen. et sp. indet., however, they combine both primitive and derived features. The facet for the atlantal intercentrum in SGM 1445–1 is wide and low as in *Grendelius alekseevi*. The anterior surface of the atlas is tuberoso and slightly concave, whereas the axial posterior surface is deeply concave. This feature is presented in *Grendelius alekseevi*, but less pronounced. The posterior edge of the humerus SGM 1554–01–11 is slightly tapered posteriorly all along its length, differing from strongly flattened edge of *Grendelius* (Fig. 15C). The humeral ‘torsion’ is caused by dorsoventral prolongation of the development of both dorsal process and deltopectoral crest as in *Sveltonectes* and *Platypterygius* (Wade 1984; McGowan and Motani 2003; Kolb and Sander 2009; Fischer et al. 2011) and unlike

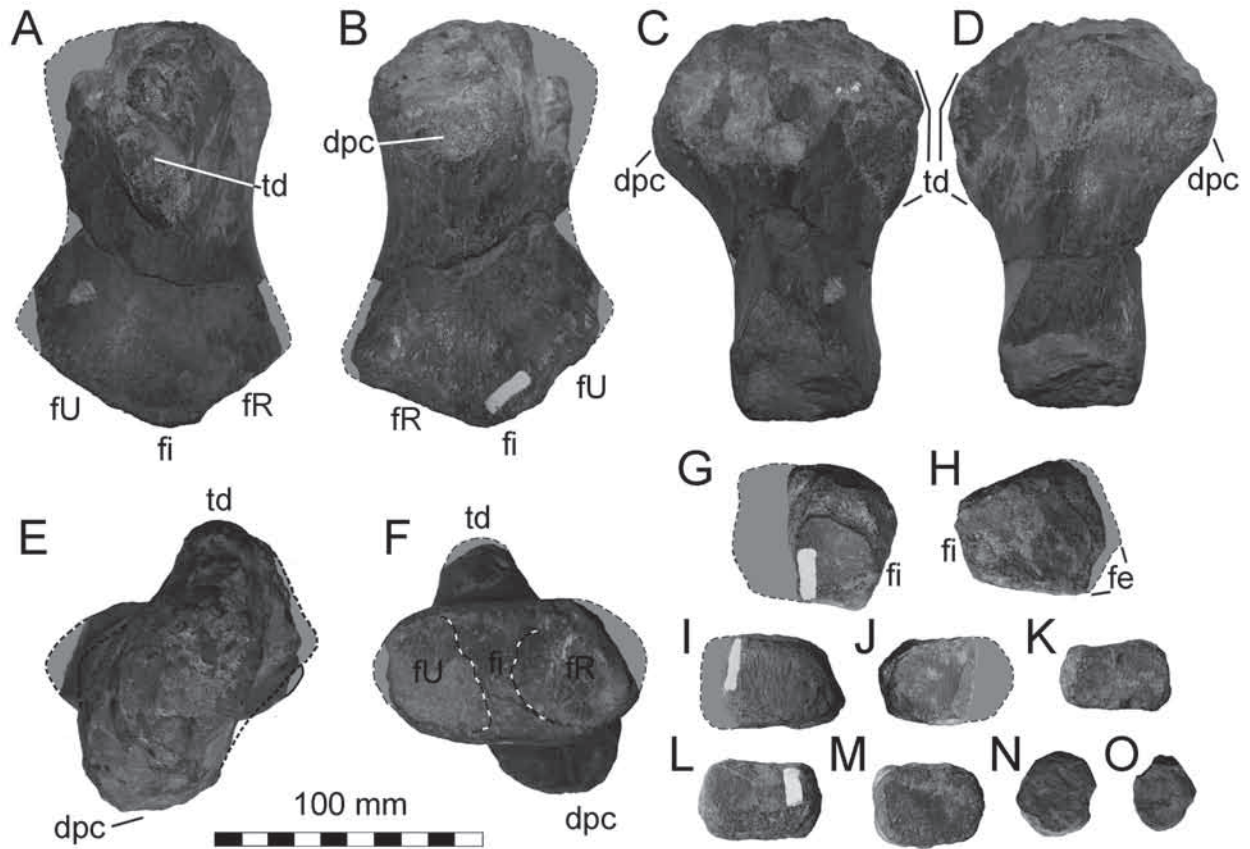


Fig. 15. Humerus and epipodium of SGM 1566: A–F – right humerus in dorsal (A), ventral (B), posterior (C), anterior (D), proximal (E) and distal (F) views; G – ulna in dorsal view; H – radius in dorsal view; elements of proximal (I–M) and distal (N, O) autopodium. For abbreviations, see Figs. 8 and 10.

Grendelius zhuravlevi and *Brachypterygius extremus* where humeral ‘torsion’ is obtained by twisting of the distal and proximal ends.

Remarks. Two triangle bite marks were partially cleared of filling sandstone on the dorsal surface of the humerus SGM 1566 (Fig. 16). The distance between them is 30 mm. Their parameters are: length 15 and 12 mm, width 6 and 5 mm. Both marks are oriented in the same direction. Judging from the shape of the marks and the distance between them, we assume that the bite could be inflicted by a medium-sized pliosaur. Triangular cross-sectioned tooth crowns are common for Late Jurassic pliosaurs (Tarlo 1960; Taylor and Cruickshank 1993; Kunsten 2012; Benson et al. 2013). Any traces of tissue regeneration are absent; this may indicate that the bites were inflicted during the deadly attack, or posthumously, during the exposure of a corpse. Predators of the higher levels in the Mesozoic seas besides hunting could also eat a floating carrion.



Fig. 16. Bite marks on the dorsal surface of the humerus SGM 1566.

Unfortunately, traces of a predation frequently cannot be distinguished from bite marks of a scavenging (Schwimmer et al. 1997). Unequivocal evidence for plesiosaur scavenging on floating corpses comes from stomach contents including dinosaurs (Taylor et al. 1993) and pterosaurs (Brown 1904). Non-fatal traumas clearly indicate hunting behavior (Zammit and Kear 2011). However, deathly bite marks are more common (Andrews 1910; Clarke and Etches 1992; Thulborn and Turner 1993; Martill 1996).

DISCUSSION

Recent data demonstrated, that presence of three distal humeral facets, one of which is for articulation with the intermedium, is not autapomorphic for the genus *Brachypterygius*, as it appears in other distinct genera: *Aegirosaurus* from the Tithonian of Germany and *Maiaspondylus* from the Albian of Canada (Bardet and Fernandez 2000; Maxwell and Caldwell 2006). As such, the synonymisation of the genera *Grendelius* and *Brachypterygius* (Maisch and Matzke 2000; McGowan and Motani 2003; Maisch 2010) should be critically re-evaluated, with detailed morphological comparison of all the elements of the paddle.

The holotype of *Brachypterygius extremus* NHMUK R317 is an associated forefin embedded in clay matrix. It was originally described as *Ichthyosaurus extremus* Boulenger, 1904. As noted herein, the precise locality and stratigraphic level of the specimen are unknown. In 1986, Delair revealed the existence of a complete left forelimb in matrix WESTM 78/219 “which, apart from coming from the opposite side of the body, is identical in virtually every respect with NHMUK R3177” (Delair 1986: 131). Next year he described BNSS 0006 as a right forefin (which we regard as a hindfin), noting that the museum data on this specimen may be inaccurate (Delair 1987).

At the moment we tend to assume that all the three specimens (limbs) are most likely representing *Brachypterygius extremus*, moreover both of the forelimbs, probably, belong to the same individual, as it was noted by Delair (1986). We suppose that there is a possibility that the hind paddle BNSS 0006 can also belong to the same individual. This suggestion is confirmed by a number of morphological and taphonomical features present in all three specimens. Morphological features include protruding far anteriorly anterodistal edge of the propodial bones, almost form-

ing a contact with the first element of the anterior accessory digit and rectangular, brick-like proximal autopodial elements possessing small notches on their ventral and dorsal borders. Taphonomical features include a sagging in the center of the autopodial elements and deformed, cracked by lithostatic pressure, posterior edges of the propodial bones.

There is a possibility that R. Damon originally obtained ichthyosaurian remains and, in his capacity as a fossil dealer, subsequently sold them separately to different buyers. In addition, our hypothesis is indirectly confirmed by similar style of preparation of all the specimens: bones are lying on the surface of clay matrix; entire specimen is fixed on the perimeter with wooden frames.

Phylogenetic analysis. The heuristic search resulted in two most parsimonious trees with a length of 134 steps, a consistency index of 0.52 and a retention index of 0.65. A strict consensus revealed two monophyletic groups, Platypterygiinae and Ophthalmosaurinae, as in Fischer et al. (2012) (Fig. 17A).

According to our analyses, *Brachypterygius extremus* and *Grendelius mordax* do not form a monophyletic group. *Grendelius* (clade ‘G’) is recovered as the basal member of Platypterygiinae (Fig. 17, clade ‘P’) and *Brachypterygius* as a member of ‘sveltonektine’ clade (clade ‘S’) (Fischer et al., 2011). Separation of *Brachypterygius* fore and hind fins into two units collapses some nodes inside Ophthalmosauridae by forming a polytomy, but confirms the position of the forefins in ‘sveltonektine’ clade and premises hindfin in the platypterygiine clade. These results seem to be consistent with our assumption.

The clade ‘G’ is supported by one unambiguous synapomorphy (character 6, state 1). The recovery of this clade, basal for Platypterygiinae (‘P’), including *Grendelius mordax*, *G. pseudoscythicus*, *G. alekseevi* and *G. zhuravlevi* is an argument in favour of synonymy of the genera *Otschevia* and *Grendelius*, what is confirmed by an almost identical morphology of the basicranium and dermatocranium in *G. alekseevi* and *G. mordax*. Some differences in the forefin architecture leave a doubt: contact of the intermedium with distal carpals 3 and 4 in BRSMG Ce 16696 (character 50, state 0), and only with distal carpal 3 in *G. pseudoscythicus*, *G. alekseevi* and *G. zhuravlevi* (derived condition for character 50). The digital bifurcation (character 53, state 1), supporting the clade with Russian species of *Grendelius*, is questionable due to absence of data on *G. zhuravlevi*.

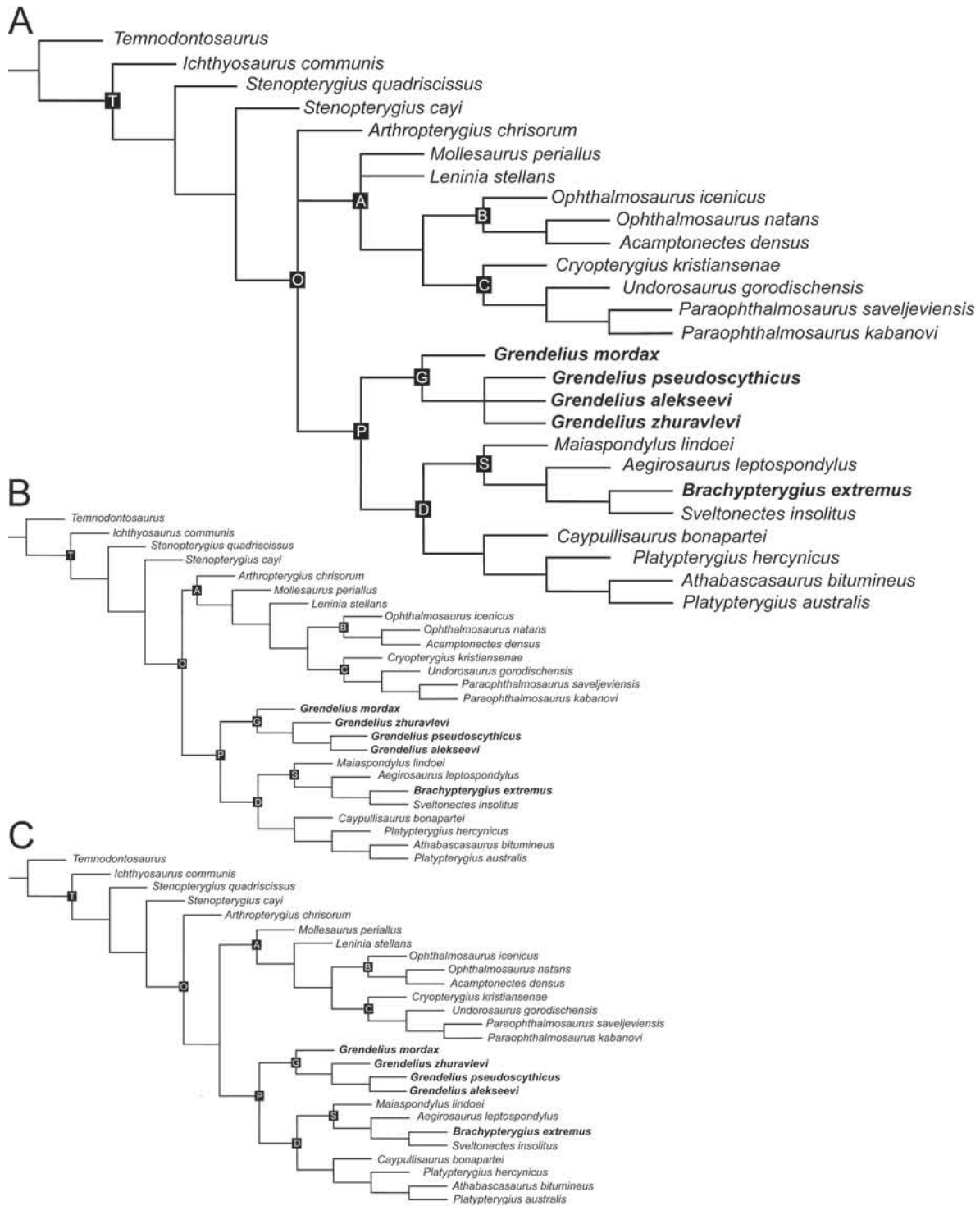


Fig. 17. Strict consensus (A) of the two most parsimonious trees (B, C) indicating the phylogenetic position of *Grendelius* and *Brachypterygius* amongst Thunnosauria. Abbreviations: T – Thunnosauria; O – Ophthalmosauridae; A – Ophthalmosaurinae; P – Platypterygiinae; B – ‘ophthalmosaurini’ clade; C – ‘paraophthalmosaurini’ clade; G – *Grendelius*; D – non-‘G’ platypterygiines; S – ‘sveltonectine’ clade.

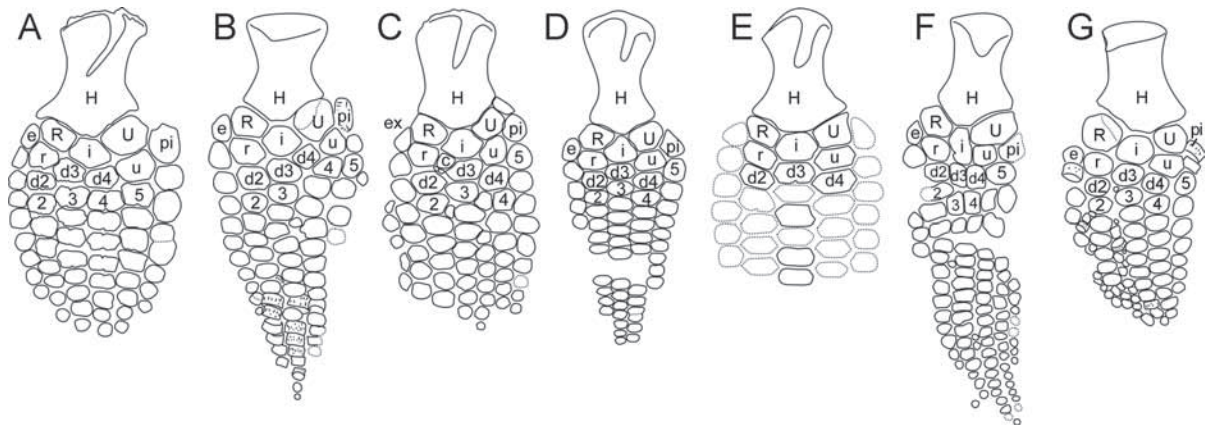


Fig. 18. Forefins of some Late Jurassic platypterygiine ophthalmosaurids: A – *Brachypterygius extremus* WESTM 78/219, left, dorsal surface (modified from Delair, 1986); B – *Grendelius mordax* BRSMG Ce 16696, right, ventral surface (based on photo provided by B.C. Moon); C – *Grendelius alekseevi* YKM 56702, left, dorsal surface; D – *Grendelius pseudoscythicus* UPM 3/100 (modified from Efimov, 1998); E – *Grendelius zhuravlevi* SRM Hb 30192, reconstruction, left, dorsal surface; F – *Aegirosaurus leptospondylus*, right, dorsal surface* (Bardet and Fernández, 2000); G – *Grendelius* sp. MJML K1747, left, ventral surface*. Images marked with an "*" are mirrored for easier comparison. For abbreviations see Fig. 8.

It is worthy mentioning the specimen MJML K1747, a partial skeleton of a young individual of *Grendelius*. This individual has a pectoral girdle and forefin architecture identical to *Grendelius pseudoscythicus* (Fig. 18) and a cranium similar to *G. mordax* and *G. alekseevi*. Such combination of features may indicate the probability of abnormal limb development in BRSMG Ce 16696 with the ulnare shifting anteroproximally during ontogenesis.

The derived platypterygiines (clade 'D') are supported by three forelimb characters: a protruding triangular deltopectoral crest (character 38, state 1), posterior enlargement of the forefin (character 47, state 1) and tightly packed rectangular phalanges (character 52, state 1)

In addition, it is worth to mention the division of Ophthalmosaurinae into two clades 'Ophthalmosaurini' – 'B' and 'Paraophthalmosaurini' – 'C'. The 'Ophthalmosaurini' clade includes *Ophthalmosaurus icenicus*, *O. natans* and *Acamptonectes densus*. It is supported by three synapomorphies: elongated paraocipital process of the opisthotic (character 23, state 1), concave posterior surface of the ulna (character 23, state 1) and latipinnate forefin architecture (character 49, state 1). The 'Paraophthalmosaurini' clade is supported by the two features: quadrangular shape of the root in cross-section (character 3, state 1) and presence of the contact of the intermedium with distal carpal 2 (character 3, state 1; unambiguous synapomorphy).

In one of the parsimonious trees *Arthropterygius* appeared to be a basal ophthalmosaurine (Fig. 17B) contra Fischer et al. (2011–2013) and Roberts et al. (2014). Such a possibility is also evidenced by recent discoveries (Zverkov et al. 2015).

ACKNOWLEDGMENTS

We sincerely thank V. Fischer (University of Liège and Royal Belgian Institute of Natural Sciences, Belgium) and J. Pardo-Pérez (Institut für Geowissenschaften, Ruprecht-Karls-Universität Heidelberg, Germany) for their critical comments, linguistic corrections and important advices on the manuscript; M. Fernández (Museo de La Plata, División Palaeontología Vertebrados, Argentina), B. Moon (University of Bristol, Bristol, UK) for provision of the important data and photo; A. Kulashova for her linguistic corrections; M. Ustinova (GIN) for microfauna and age identification; V. Kosorukov (MSU) for matrix X-ray phase analysis; I. Starodubtseva (SGM), O. Borodina (YKM) and N. Panteeva (SRM) for their help that makes our study of the material as easy as possible. We appreciate P. Skutschas and one anonymous reviewer for their comments and recommendations that improved this work. We also thank the SGM, YKM and SRM staff for their help during our work there.

REFERENCES

Andrews C.W. 1910. A descriptive catalogue of the marine reptiles of the Oxford clay. Part. I. Trustees of the British Museum. London, 205 p.

- Appleby R.M. 1956.** The osteology and taxonomy of the fossil reptile *Ophthalmosaurus*. *Proceedings of the Zoological Society of London* **126**: 403–447.
- Arkhangelsky M.S. 1997.** On a new ichthyosaurian genus from the Lower Volgian substage of the Saratov, Volga region. *Paleontological Journal*, **31**(1): 87–91.
- Arkhangelsky M.S. 1998a.** On the ichthyosaurian fossils from the Volgian stage of the Saratov Region. *Paleontological Journal*, **32**(2): 192–196.
- Arkhangelsky M.S. 1998b.** Mesozoic marine reptiles of the Volga Region near Saratov, and their stratigraphic and bionomic significance. Ph.D. thesis. Saratov State University, Saratov, 261 p. [In Russian].
- Arkhangelsky M.S. 2000.** On the ichthyosaur *Otschevia* from the Volgian stage of the Volga Region. *Paleontological Journal*, **34**(5): 549–552.
- Arkhangelsky M.S. 2001.** On a new ichthyosaur of the genus *Otschevia* from the Volgian stage of the Volga region near Ulyanovsk. *Paleontological Journal*, **35**(6): 629–634.
- Arkhangelsky M.S. 2008.** Subclass Ichthyopterygia. In: M.F. Ivakhnenko and E.N. Kurochkin (Eds.). Fossil vertebrates of Russia and neighboring countries. Fossil reptiles and birds. Part 1. GEOS, Moscow: 244–262. [In Russian].
- Arkhangelsky M.S., Averianov A.O., Pervushov E.M., Ratnikov V.Y. and Zozyrev N.Y. 2008.** On ichthyosaur remains from the Cretaceous of the Voronezh region. *Palaeontological Journal*, **42**: 287–291.
- Arkhangelsky M.S. and Zverkov N.G. 2014.** On a new ichthyosaur of the genus *Undorosaurus*. *Proceedings of the Zoological Institute*, **318**(3): 187–196.
- Bardet N. and Fernandez M. 2000.** A new ichthyosaur from the Upper Jurassic lithographic limestones of Bavaria. *Journal of Paleontology*, **74**: 503–511.
- Benson R.B.J., Evans M., Smith A.S., Sassoon J., Moore-Faye S., Ketchum H.F. and Forrest R. 2013.** A giant pliosaurid skull from the Late Jurassic of England. *PLoS ONE*, **8**(5): e65989.
- Boulenger G.A. 1904.** On a new species of ichthyosaur from Bath. *Proceedings of the Zoological Society of London*, **1904**(1): 424–426. [Title on reprint].
- Brown B. 1904.** Stomach stones and food of plesiosaurs. *Science (N.S.)*, **20**(501):184–185.
- Buchy M.-C. and López Oliva J. G. 2009.** Occurrence of a second ichthyosaur genus (Reptilia: Ichthyosauria) in the Late Jurassic Gulf of Mexico. *Boletín de la Sociedad Geológica Mexicana*, **61**: 233–238.
- Carroll R.L. and Dong Z. 1991.** *Hupehsuchus*, an enigmatic aquatic reptile from the Triassic of China, and the problem of establishing relationships. *Philosophical Transactions of the Royal Society B: Biological Sciences*, **331**: 131–153.
- Chen X-h., Motani R., Cheng L., Jiang D-y. and Rieppel O. 2014.** A carapace-like bony ‘body tube’ in an Early Triassic marine reptile and the onset of marine tetrapod predation. *PLoS ONE*, **9**(4): e94396.
- Clarke J.B. and Etches S.M. 1992.** Predation amongst Jurassic marine reptiles. *Proceedings of the Dorset Natural History and Archaeology Society*, **113**: 202–205.
- Delair J.B. 1986.** Some little known Jurassic ichthyosaurs from Dorset. *Proceedings of the Dorset Natural History and Archaeological Society*, **107**: 127–134.
- Delair J.B. 1987.** An unusual ichthyosaurian forelimb from Rodwell, Dorset. *Proceedings of the Dorset Natural History and Archaeology Society*, **108**: 210–212.
- Druckenmiller P.S. and Maxwell E.E. 2010.** A new Lower Cretaceous (lower Albian) ichthyosaur genus from the Clearwater Formation, Alberta, Canada. *Canadian Journal of Earth Sciences*, **47**: 1037–1053.
- Druckenmiller P.S., Hurum J.H., Knutsen E.M. and Næskrem H.A. 2012.** Two new ophthalmosaurids (Reptilia: Ichthyosauria) from the Agardhfjellet Formation (Upper Jurassic: Volgian/Tithonian), Svalbard, Norway. *Norwegian Journal of Geology*, **92**: 311–339.
- Efimov V.M. 1997.** The Late Jurassic and Early Cretaceous ichthyosaurs of Middle Volga and Moscow regions: systematics, stratigraphic distribution, taphonomy. Ph.D. thesis. Saratov State University, Saratov, 182 p. [In Russian].
- Efimov V.M. 1998.** An ichthyosaur, *Otschevia pseudocythica* gen. et sp. nov. from the Upper Jurassic strata of the Ulyanovsk region. *Paleontological Journal*, **32**(2): 187–191.
- Efimov V.M. 1999a.** Ichthyosaurs of a new genus *Yasykovia* from the Upper Jurassic strata of European Russia. *Paleontological Journal*, **33**(1): 91–98.
- Efimov V.M. 1999b.** A new family of ichthyosaurs, the Undorosauridae fam. nov. from the Volgian stage of the European part of Russia. *Paleontological Journal*, **33**(2): 174–181.
- Fernández M.S. 1994.** A new long-snouted ichthyosaur from the Early Bajocian of Neuquén Basin (Argentina). *Ameghiniana*, **31**: 291–297.
- Fernández M.S. 1997.** A new ichthyosaur from the Tithonian (Late Jurassic) of the Neuquén Basin, North-western Patagonia, Argentina. *Journal of Paleontology*, **71**(3): 479–484.
- Fernández M.S. 1999.** A new ichthyosaur from the Los Molles Formation (Early Bajocian), Neuquen Basin, Argentina. *Journal of Paleontology*, **73**(4): 677–681.
- Fernández M.S. 2001.** Dorsal or ventral? Homologies of the forefin of *Caypullisaurus* (Ichthyosauria: Ophthalmosauria). *Journal of Vertebrate Paleontology* **21**: 515–520.
- Fernández M.S. 2007.** Redescription and phylogenetic position of *Caypullisaurus* (Ichthyosauria: Ophthalmosauridae). *Journal of Paleontology* **81**: 368–375.
- Fernández M. S. and Talevi M. 2014.** Ophthalmosaurian (Ichthyosauria) records from the Aalenian–Bajocian of

- Patagonia (Argentina): an overview. *Geological Magazine*, **151**: 49–59.
- Fischer V. 2012.** New data on the ichthyosaur *Platypterygius hercynicus* and its implications for the validity of the genus. *Acta Palaeontologica Polonica*, **57**(1):123–134.
- Fischer V., Masure E., Arkhangelsky M.S. and Godefroit P. 2011.** A new Barremian (Early Cretaceous) ichthyosaur from western Russia. *Journal of Vertebrate Paleontology*, **31**(5): 1010–1025.
- Fischer V., Maisch M.W., Naish D., Kosma R., Liston J., Joger U., Krüger F.J., Fritz J., Pardo Pérez J., Tainsh J. and Appleby R. 2012.** New ophthalmosaurid ichthyosaurs from the European Lower Cretaceous demonstrate extensive ichthyosaur survival across the Jurassic–Cretaceous boundary. *PLoS ONE*, **7**(1): e29234.
- Fischer V., Arkhangelsky M.S., Uspensky G.N., Stenshin I.M. and Godefroit P. 2014a.** A new Lower Cretaceous ichthyosaur from Russia reveals skull shape conservatism within Ophthalmosaurinae. *Geological Magazine*, **151**(1): 60–70.
- Fischer V., Bardet N., Guiomar M. and Godefroit P. 2014b.** High Diversity in Cretaceous Ichthyosaurs from Europe Prior to Their Extinction. *PLoS ONE* **9**(1): e84709.
- Fischer V., Arkhangelsky M.S., Naish D., Stenshin I.M., Uspensky G.N. and Godefroit P. 2014c.** *Simbirskiasaurus* and *Pervushoviasaurus* reassessed: implications for the taxonomy and cranial osteology of Cretaceous platypterygiine ichthyosaurs. *Zoological Journal of the Linnean Society*, **171**: 822–841.
- Gilmore C.W. 1905.** Osteology of *Baptanodon* (Marsh). *Memoirs of the Carnegie Museum*, **2**(2): 77–129.
- Goloboff P., Farris, J. and Nixon K. 2008.** TNT, a free program for phylogenetic analysis. *Cladistics*, **24**: 774–786.
- Huene F. von. 1922.** Die Ichthyosaurier des Lias und ihre Zusammenhänge. Berlin: Verlag von Gebrüder Borntraeger, 114 p.
- Johnson R. 1979.** The osteology of the pectoral complex of *Stenopterygius* Jaekel Reptilia: Ichthyosauria. *Neues Jahrbuch fuer Geologie und Palaeontologie Abhandlungen*, **159**(1): 41–86.
- Kear B.P. 2005.** Cranial morphology of *Platypterygius longmani* Wade, 1990 (Reptilia: Ichthyosauria) from the Lower Cretaceous of Australia. *Zoological Journal of the Linnean Society*, **145**: 583–622.
- Kirton A.M. 1983.** A review of British Upper Jurassic ichthyosaurs. Ph.D. thesis, University of Newcastle-upon-Tyne, 239 p.
- Kolb C. and Sander P.M. 2009.** Redescription of the ichthyosaur *Platypterygius hercynicus* (Kuhn, 1946) from the Lower Cretaceous of Salzgitter (Lower Saxony, Germany). *Palaeontographica Abteilung a-Palaeozoologie-Stratigraphie*. **288**: 151–192.
- Knutsen E.M. 2012.** A taxonomic revision of the genus *Phiosaurus* (Owen, 1841a) Owen, 1841b. *Norwegian Journal of Geology*, **92**: 259–276.
- Maisch M.W. and Matzke A.T. 2000.** The Ichthyosauria. *Stuttgarter Beitrage zur Naturkunde, Serie B*, **298**: 1–159.
- Maisch M.W. 2010.** Phylogeny, systematics, and origin of the Ichthyosauria – the state of the art. *Palaeodiversity*, **3**: 151–214;
- Martill D.M. 1996.** Fossils explained: ichthyosaurs. *Geology Today*, **12**: 194–196.
- Maxwell E.E. 2010.** Generic reassignment of an ichthyosaur from the Queen Elizabeth Islands, Northwest Territories, Canada. *Journal of Vertebrate Paleontology*, **2**(30): 403–415.
- Maxwell E.E. and Caldwell M.W. 2006.** A new genus of ichthyosaur from the Lower Cretaceous of Western Canada. *Palaeontology*, **49**: 1043–1052.
- Maxwell E.E. and Kear B.P. 2010.** Postcranial anatomy of *Platypterygius americanus* (Reptilia: Ichthyosauria) from the Cretaceous of Wyoming. *Journal of Vertebrate Paleontology*, **30**: 1059–1068.
- Maxwell E.E., Zammit M. and Druckenmiller P.S. 2012.** Morphology and orientation of the ichthyosaurian femur. *Journal of Vertebrate Paleontology*, **32**(5): 1207–1211.
- Maxwell E.E., Dick D., Padilla S. and Parra M.L. 2015.** A new ophthalmosaurid ichthyosaur from the Early Cretaceous of Colombia. *Papers in Palaeontology*. doi: 10.1002/spp2.1030
- McGowan C. 1976.** The description and phenetic relationships of a new ichthyosaur genus from the Upper Jurassic of England. *Canadian Journal of Earth Sciences*, **13**: 668–683.
- McGowan C. 1997.** The taxonomic status of the Late Jurassic ichthyosaur *Grendelius mordax*: a preliminary report. *Journal of Vertebrate Paleontology*, **17**: 428–430.
- McGowan C. and Motani R. 2003.** Ichthyopterygia. In H.-D. Sues (Ed.), *Handbook of Paleoherpptology*. Part 8. Verlag Dr. Fr. Pfeil, Munchen: 1–178.
- Motani R., Jiang D.-Y., Tintori A., Rieppel O., Chen G. B. and You H. 2015.** First evidence of centralia in Ichthyopterygia reiterating bias from paedomorphic characters on marine reptile phylogenetic reconstruction. *Journal of Vertebrate Paleontology*, **35**(4): e948547.
- Pervushov E.M., Arkhangelsky M.S. and Ivanov A.V. 1999.** Catalogue of localities of marine reptiles in the Jurassic and Cretaceous deposits of the Lower Volga region. College, Saratov, 230 p. [In Russian].
- Roberts A.J., Druckenmiller P.S., Sætre G.-P. and Hurum J.H. 2014.** A new Upper Jurassic ophthalmosaurid ichthyosaur from the Slottsmøya Member, Agardhfjellet Formation of Central Spitsbergen. *PLoS ONE* **9**(8): e103152.
- Sander P. M. 2000.** Ichthyosauria: their diversity, distribution, and phylogeny. *Palaeontologische Zeitschrift*, **74**: 1–35.

- Shubin N.H. and Alberch P. 1986.** A morphogenetic approach to the origin and basic organization of the tetrapod limb. In: M.K. Hecht, B. Wallace, and G.T. Prance (Eds.). *Evolutionary Biology*, Vol. 20. Plenum Press, New York and London: 319–387.
- Schwimmer D.R., Steward J.D. and Williams G.D. 1997.** Scavenging by sharks of the genus *Squalicorax* in the Late Cretaceous of North America. *Palaios*, 12: 71–73.
- Stepanov S.A., Arkhangelsky M.S. and Ivanov A.V. 2004.** On paleopathology of Ichthyopterygia. Transactions of the Scientific Research Geological Institute of the N.G. Chernyshevskii Saratov State University, New Series. 14: 163–171.
- Storrs G.W., Arkhangel'skii M.S. and Efimov V.M. 2000.** Mesozoic marine reptiles of Russia and other former Soviet republics. In: M.J. Benton, M.A. Shishkin, D.M. Unwin and E.N. Kurochkin (Eds.). *The age of dinosaurs in Russia and Mongolia*. Cambridge University Press, Cambridge: 187–210.
- Tarlo L.B. 1960.** A review of the Upper Jurassic pliosaurs. *Bulletin of the British Museum (Natural History), Geology Series*, 4: 147–189.
- Taylor M.A. and Cruickshank A.R.I. 1993.** Cranial anatomy and functional morphology of *Pliosaurus brachyspondylus* (Reptilia: Plesiosauria) from the Upper Jurassic of Westbury, Wiltshire. *Philosophical Transactions of the Royal Society of London*, B 341: 399–418.
- Taylor M.A., Norman D.B. and Cruickshank A.R.I. 1993.** Remains of an ornithischian dinosaur in a pliosaur from the Kimmeridgian of England. *Palaeontology*, 36: 357–360.
- Thulborn R.A. and Turner S. 1993.** An elasmosaur bitten by a pliosaur. *Modern Geology*, 18: 489–501.
- Wade M. 1984.** *Platypterygius australis*, an Australian Cretaceous ichthyosaur. *Lethaia*, 17: 99–113.
- Wade M. 1990.** A review of the Australian Cretaceous longipinnate ichthyosaur *Platypterygius* (Ichthyosauria, Ichthyopterygia). *Memoirs of the Queensland Museum*, 28: 115–137.
- Zammit M. and Kear B. 2011.** Healed bite marks on a Cretaceous ichthyosaur. *Acta Palaeontologica Polonica*, 56(4): 859–863.
- Zammit M., Norris R.M. and Kear B.P. 2010.** The Australian Cretaceous ichthyosaur *Platypterygius australis*: a description and review of postcranial remains. *Journal of Vertebrate Paleontology*, 30: 1726–1735.
- Zverkov N.G., Arkhangelsky M.S., Pardo Pérez J.M. and Beznosov P.A. 2015.** On the Upper Jurassic ichthyosaur remains from the Russian North. *Proceedings of the Zoological Institute of the Russian Academy of Sciences*, 319(1): 81–97.

Submitted January 28, 2015; accepted December 1, 2015.

APPENDIX 2. Description of characters used in the phylogenetic analysis. The characters are modified from those provided by Fischer et al. (2012, 2014a, 2014c) and the references therein. The characters 11, 13, 24, 33, 35, 40, 49, 56 are modified from Arkhangel'sky and Zverkov (2014; characters 52–54), Sander (2000; characters 10, 83, 93) and Roberts et al. (2014; characters 12, 25, 52). The New characters (7, 27) are indicated with an ‘*’.

1. Crown striation: presence of deep longitudinal ridges (0); crown enamel subtly ridged or smooth (1).
2. Base of enamel layer: poorly defined, invisible (0); well defined, precise (1).
3. Shape of the root in cross-section in adults: rounded (0); quadrangular (1).
4. Processus postpalatinis pterygoidei: absent (0); present (1).
5. Maxilla anterior process: extending anteriorly as far as nasal or further anteriorly (0); reduced (1).
6. Descending process of the nasal on the dorsal border of the nares: absent (0); present (1); contacts the maxilla, dividing the naris in two (regardless of the reduction of the anterior naris) (2).
7. *Process of the nasal overlaps externally premaxilla no (0); yes (1).
8. Processus narialis of the maxilla in lateral view: absent (0); present (1).
9. Processus supranarialis of the premaxilla: present (0); absent or reduced (1).
10. Processus narialis of the prefrontal: present (0); absent (1).
11. Anterior margin of the jugal: tapering, running between lacrimal and maxilla (0); broad and fan-like, covering large are of maxilla venterolaterally (1).
12. Posterior margin of the jugal: articulates with the postorbital and quadratojugal (0); excluded from the quadratojugal by the postorbital (1) (Character 12 in Roberts et al. 2014).
13. Lacrimale participation in the posterior border of the external nares: yes (0); no, lacrimale is excluded from the posterior border of the nares by maxilla (1). (Character 10 from Sander, 2000).
14. Sagittal eminence: present (0); absent (1).
15. Processus temporalis of the frontal: absent (0); present (1).
16. Supratemporal-postorbital contact: absent (0); present (1).
17. Squamosal shape: triangular (0); squared (1); squamosal absent (2).
18. Quadratojugal exposure: extensive (0); small, largely covered by squamosal or supratemporal and postorbital (1).
19. Basiopterygoid processes: short, giving basisphenoid a square outline in dorsal view (0); markedly expanded laterally, being wing-like, giving basisphenoid a marked pentagonal shape in dorsal view (1).
20. Extracondylar area of basioccipital: wide (0); reduced but still present ventrally and lateral (1); extremely reduced, being nonexistent at least ventrally (2).
21. Basioccipital peg: present (0); absent (1).
22. Ventral notch in the extracondylar area of the basioccipital: present (0); absent (1).
23. Shape of the paroccipital process of the ophisthotic: short and robust (0); elongated and slender (1).
24. Stapes proximal head: slender, much smaller than opisthotic proximal head (0); massive, as large or larger than opisthotic head (1).
25. Stapedial shaft in adults: thick (0); slender and gracile (1). (Character 25 in Roberts et al. 2014).
26. Angular lateral exposure: much smaller than surangular exposure (0), extensive (1).
27. *Ventral keel on atlas-axis complex, bordered laterally by a concave areas: no, ventral keel is rounded (0); yes (1).
28. Posterior dorsal/anterior caudal centra: 3.5 times or less as high as long (0); four times or more as high as long (1).
29. Tail fin centra: strongly laterally compressed (0); as wide as high (1).
30. Neural spines of atlas-axis: completely overlapping, may be fused (0), never fused (1).
31. Chevrons in apical region: present (0); lost (1).
32. Glenoid contribution of the scapula: extensive, being at least as large as the coracoid facet (0); reduced, being markedly smaller than the coracoid facet (1).
33. Prominent acromion process of scapula: absent (0); present (1).

34. Coracoid shape in adults: (0) rounded (length to width ratio less than 1,3, and often is close to 1); (1) elongated (length to width ratio greater than or equal to 1,5). (Character 52 in Arkhangelsky and Zvekov, 2014).
35. Anteromedial process of coracoid and anterior notch: present (0); absent (1).
36. Medial facet for the scapula on anteromedial process of coracoid: 0 – absent, 1 – present and well prominent. (Character 53 in Arkhangelsky and Zvekov, 2014).
37. Plate-like dorsal ridge on humerus: absent (0); present (1).
38. Protruding triangular deltopectoral crest on the humerus: absent (0); present (1). (modified by Roberts et al. 2014).
39. Humerus distal and proximal ends in dorsal view: distal end wider than proximal end (0), nearly equal or proximal end slightly wider than distal end (1).
40. Humerus posterior edge in adults: rounded (0) flattened and blade-like all along its length (1) (Modification of character 83 from Sander, 2000).
41. Humerus anterodistal facet for preaxial accessory element anterior to radius; absent (0); present (1).
42. Humerus with posterodistally deflected ulnar facet and distally facing radial facet: no (0); yes (1).
43. Humerus/intermedium contact: absent (0); present (1).
44. Shape of the posterior surface of the ulna: rounded or straight and nearly as thick as the rest of the element (0); concave and edgy (1).
45. Manual pisiform: absent (0), present (1).
46. Notching of anterior facet of leading edge elements of forefin in adults: present (0); absent (1).
47. Posterior enlargement of forefin: number of postaxial accessory 'complete' digits: none (0); one (1), two or more (2).
48. Preaxial accessory digits on forefin: absent (0); present (1).
49. Longipinnate or latipinnate forefin architecture: posterodistal (0); distal (1) contact of ulnare with metacarpal 5.
50. Intermedium/distal carpals contact: (0), with dc 3,4; (1), with dc 2,3; (2), with dc 3 (Modification of char. 54 from Arkhangelsky and Zvekov, 2014; it is now resembles character 93 from Sander, 2000)
51. Zeug- to autopodial elements flattened and plate-like (0); strongly thickened (1).
52. Tightly packed rectangular phalanges: absent, phalanges are mostly rounded (0), present (1).
53. Digital bifurcation: absent (0); frequently occurs in digit IV (1).
54. Ischium-pubis fusion in adults: absent or present only proximally (0); present with an oburator foramen (1); present with no oburator foramen (2).
55. Ischium or ischiopubis shape: plate-like, flattened (0); rod-like (1).
56. Prominent, ridge-like dorsal and ventral process demarked from the head of the femur and extending up to the mid-shaft: absent (0); present (1).
57. Ventral process on femur: smaller than dorsal process (0), more prominent (1). (Char. 52 in Roberts et al. 2014)
58. Astragalus/femoral contact: absent (0); present (1).
59. Femur anterodistal facet for accessory zeugopodial element anterior to tibia: absent (0); present (1).
60. Tibia peripheral shaft in adults: notched (0); straight (1).
61. Postaxial accessory digit: absent (0); present (1).

APPENDIX 3. Discussion of some characters.

The character 49 (originally 41) from Fischer et al. (2012) based on intermedium with distal carpals contact is unable to characterize all variants of forefine architecture, however we can confidently distinguish two types of forefins (longipinnate and latipinnate forefins) based on contact of the ulnare with metacarpal 5, which can be either posterodistal (in longipinnate fin), or distal (in latipinnate fins).

The character 50 (54 in Arkhangelsky and Zvekov [2014] and 93 in Sander [2000], instead of character 49 (41 in Fischer et al. [2012])) describes various configurations of intermedium to distal carpals contact.

Character states changed for *Caypullisaurus bonapartei* according Fernandez (2007: 6 (0–1), 11 (?–1), 15–(?–1), 47 – (2–1) (NZ interpretation).

According Fernandez and Talevi, 2013 some character states were changed for *Mollesaurus periallus*: 1 (?–0); 2 (?–1); 3 (?–0); 4 (?–0); 11 (?–1).

According Roberts et al., 2014 we accept changing of character states for *Arthropterygius*: 21 (here 24) (1–?); 40 (48) (?–1); 42 (51) (?–1); 43(52) (?–0); 49(59) (?–0) and do not accept their changes for characters: 32(39) (1–0) and 47(56) (0–1).

We do not accept changing of character states by Roberts et al., 2014 for *Caypullisaurus* from Fischer *et al.* 2012: 45 (here 55) and 46 (56). Because we believe, that the element (Fernandez 2007, fig 2) is ishiopubis and possesses the characteristics correctly encoded by Fischer et al., 2012.

We reserve the coding of character states for *Undorosaurus* and *Cryopterygius* as in Arkhangelsky and Zverkov, 2014 and do not accept some differences existing in Roberts et al., 2014.

New characters:

The character 7 was added in order to describe the unique feature of the genus *Grendelius*, having a flattened outgrowth of the nasal, which overlaps premaxilla externally.

In the character 27 we describe the distinct feature of advanced platypterygiinae ichthyosaurs – ventral kille on atlas-axis complex, which is bordered laterally by concave areas.